Journal Pre-proof

Design, synthesis and structure–activity relationship of indolylindazoles as potent and selective covalent inhibitors of interleukin-2 inducible T-cell kinase (ITK)

Xueying wang, Gang Xue, Zhengying Pan

Please cite this article as: X. wang, G. Xue, Z. Pan, Design, synthesis and structure–activity relationship of indolylindazoles as potent and selective covalent inhibitors of interleukin-2 inducible T-cell kinase (ITK), *European Journal of Medicinal Chemistry* (2019), doi: https://doi.org/10.1016/j.ejmech.2019.111918.

This is a PDF file of an article that has undergone enhancements after acceptance, such as the addition of a cover page and metadata, and formatting for readability, but it is not yet the definitive version of record. This version will undergo additional copyediting, typesetting and review before it is published in its final form, but we are providing this version to give early visibility of the article. Please note that, during the production process, errors may be discovered which could affect the content, and all legal disclaimers that apply to the journal pertain.

20a
ITK IC$_{50}$= 102 nM

21
ITK IC$_{50}$= 64 nM

27
ITK IC$_{50}$= 5.6 nM
BTK/ITK= 4.5×

43
ITK IC$_{50}$= 4.0 nM, BTK/ITK= 33×
pPLC-γ1 in Jurkat, EC$_{50}$= 119 nM
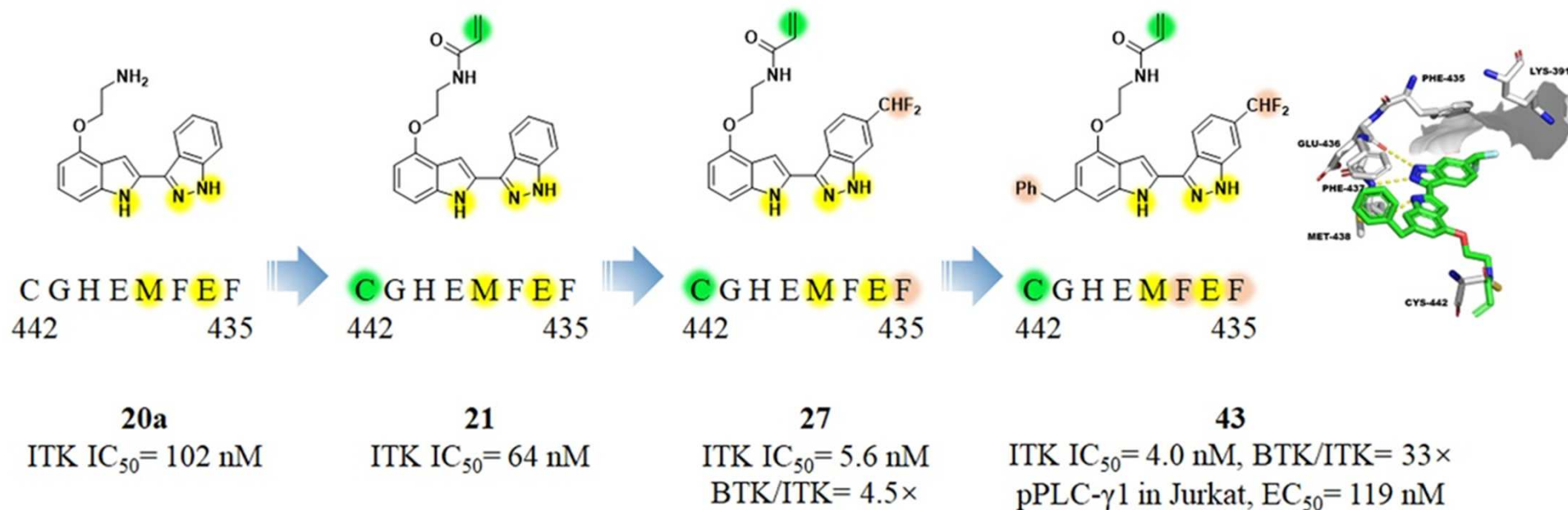
A novel series of potent covalent ITK inhibitor were developed based on the indolylindazole scaffold.

Design, synthesis and structure–activity relationship of indolylindazoles as potent and selective covalent inhibitors of interleukin-2 inducible T-cell kinase (ITK)

Xueying wang, Gang Xue, Zhengying Pan*

State Key Laboratory of Chemical Oncogenomics, Engineering Laboratory for Chiral Drug Synthesis, School of Chemical Biology and Biotechnology, Shenzhen Graduate School, Peking University, Shenzhen, 518055, China

Keywords: ITK, tyrosine kinase, covalent inhibitor, T-cell receptor, indolylindazole

Abstract

Interleukin-2 inducible T-cell kinase (ITK), a member of the Tec family of tyrosine kinases, plays an important role in T cell signaling downstream of the T-cell receptor (TCR). Herein we report the discovery of a series of indolylindazole based covalent ITK inhibitors with nanomolar inhibitory potency against ITK, good kinase selectivity and potent inhibition of the phosphorylation of PLCγ1 and ERK1/2 in living cells. A computational study provided insight into the interactions between inhibitors and Phe437 at the ATP binding pocket of ITK, suggesting that both edge-to-face π-π interaction and the dihedral torsion angle contribute to inhibitors' potency. Compounds **43** and **55** stood out as selective covalent inhibitors with potent cellular activity, which could be used as chemical tools for further study of ITK functions.

1. Introduction

Interleukin-2 inducible T-cell kinase (ITK) is a member of the Tec family of nonreceptor protein tyrosine kinases. This family consists of five members: Bruton's tyrosine kinase (BTK), ITK, resting lymphocyte kinase (RLK), tyrosine kinase expressed in hepatocellular carcinoma (TEC) and bone marrow tyrosine kinase in chromosome x (BMX) [1]. Only ITK, RLK and TEC are expressed in T cells, and ITK has a predominant role in the T-cell receptor (TCR) signaling pathway [2]. In ITK knock-out cells, phospholipase Cγ-1 (PLCγ1) activation is decreased, leading to diminished Ca^{2+} flux and reduced mitogen-associated protein kinase (MAPK) activation, resulting in defective activation of downstream signaling molecules including the nuclear factor for activated T cells (NFAT) and activator protein-1 (AP-1) [3, 4]. ITK also plays an important role in the secretion of pro-inflammatory cytokines, such as IL-2, IL-4, IL-5 and IL-13 [5]. Due to its critical role in T cell signaling, ITK is an appealing therapeutic target for allergic, autoimmune, inflammatory, infectious and neoplastic diseases [6, 7]. Studies have shown that ITK-deficient mice are more vulnerable to drastically reduced lung inflammation, eosinophil infiltration and mucous production in response to ovalbumin-induced allergic asthma [8]. ITK could affect the infection and replication of HIV [9, 10], and ITK mutations have been reported in patients with EBV-associated lymphoproliferative diseases that may be related to an impaired cytotoxic CD8^{+} T cell response [11]. In addition, CD28-ITK signals specifically regulate self-reactive T cell migration in tissues. Small molecule inhibitors of ITK have been reported to reduce T cell infiltration and destroy islet cells in mouse models of type I diabetes [12]. Moreover, ITK is a critical signaling component in acute lymphoblastic T-cell leukemia and cutaneous T-cell lymphoma due to its aberrant activation and upregulated expression [13, 14].

During the past few decades, a number of ITK inhibitors have been disclosed (Fig. 1), most of which are reversible ATP-competitive inhibitors binding in the active conformation of ITK. For example, Bristol-Myers Squibb early reported a potent aminothiazole ITK inhibitor BMS-509744 (**1**) [15, 16]. Subsequently, more ITK inhibitors based on a variety of chemical scaffolds (**2**–**8**) were discovered by pharmaceutical companies and academic research groups [10, 16-29]. It is worth mentioning that Japan Tobacco has progressed JTE-051 into

phase II clinical trials for the treatment of rheumatoid arthritis (NCT02919475), but the chemical structure and discovery of JTE-051 itself have not been disclosed. Irreversible ITK inhibitors (**9**–**11**) [19-21] have been developed through covalent bonding with a noncatalytic cysteine residue (Cys442) located in the ATP-binding pocket of the kinase. There are only ten other kinases in the human kinome that possess a cysteine residue at the same position as Cys442 in ITK, including TEC family (TEC, ITK, BTK, RLK), EGFR family (EGFR, HER2, HER4), BLK, JAK3 and MAP2K7. Due to the conserved nature of the ATP-binding site, developing highly selective ATP-competitive kinase inhibitors is a great challenge. Targeting a rare amino acid residue of a kinase with covalent inhibitors is an innovative approach for achieving selective kinase inhibitors [22, 23]. Covalent ITK inhibitors also have the potential to overcome competition from the high ATP concentration in the native cellular environment and prolong the inhibition effect of the TCR pathway [19]. Despite years of efforts, there has been little active progress for ITK inhibitors in clinical trials, especially given that no covalent ITK inhibitor has entered a clinical trial. Thus, more efforts in developing ITK inhibitors are in much need. Our research group has recently disclosed our efforts in developing 7*H*-pyrrolo[2,3-*d*]pyrimidine based ITK inhibitors (**12**) [24]. Herein, we report the design, synthesis and structure-activity relationship (SAR) studies of another novel class of potent covalent ITK inhibitors based on an indolylindazole scaffold.
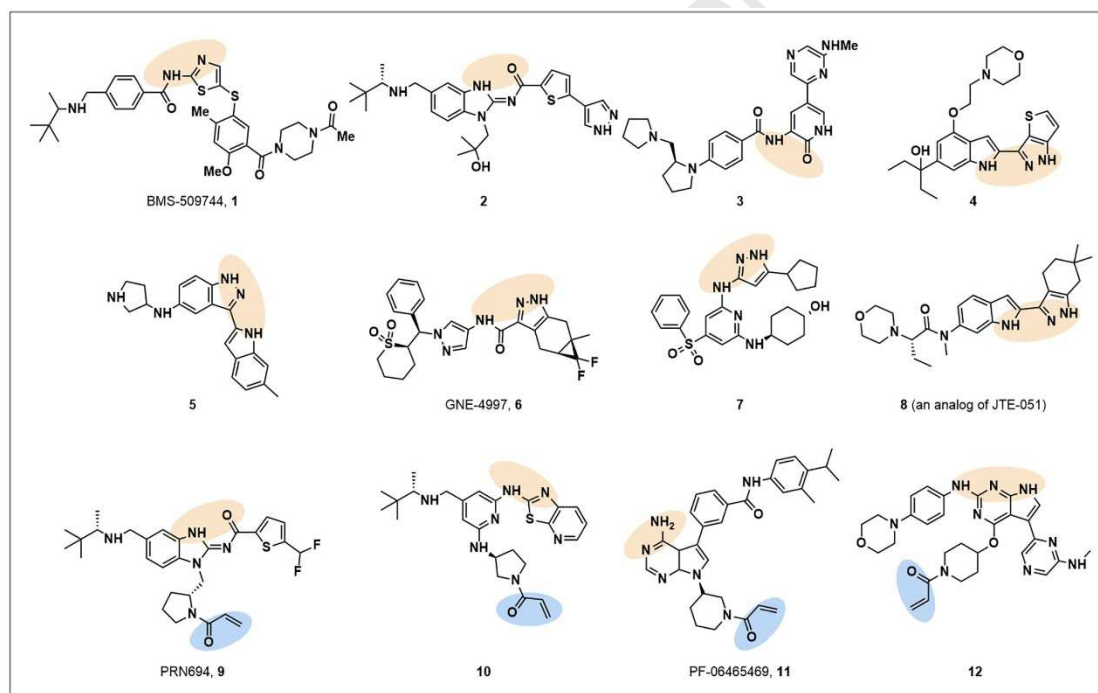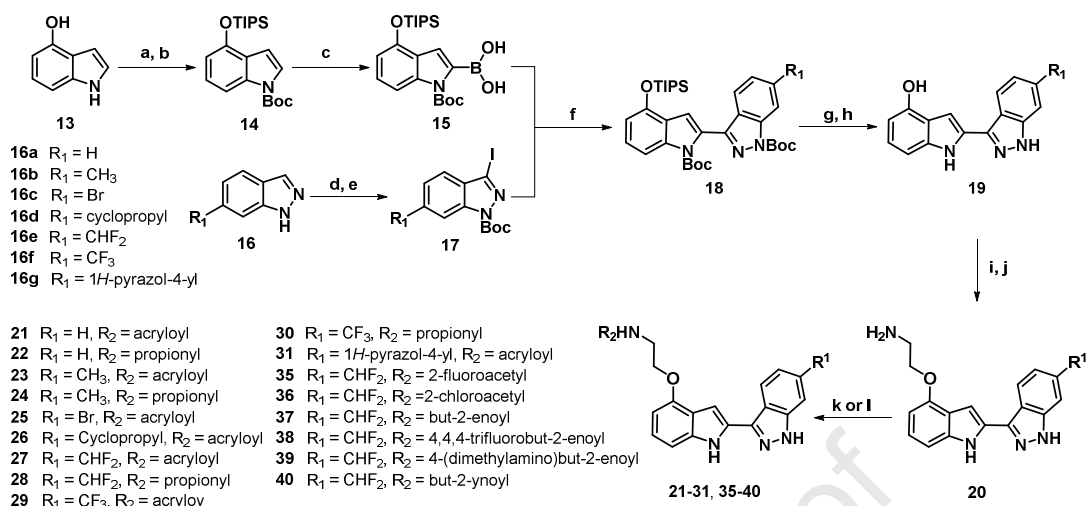

Fig. 1. Representative ITK inhibitors. Atoms participating in direct hydrogen bonding to the hinge region of the ATP site are highlighted in orange and the electrophilic warheads are highlighted in blue.

2. Chemistry

The synthetic route for preparing indolylindazole derivatives is described in Scheme 1 [25]. Starting from commercially available 1*H*-indol-4-ol **13**, boronic acid **15** was prepared by sequential protection steps with Boc and TIPS groups, followed by a borylation reaction. Iodo-compound **17** was prepared by regioselective iodination of indazole **16** followed by Boc protection. The key intermediate **18** was produced via Suzuki coupling of **15** and **17**, which went through subsequent deprotection procedures to furnish compound **19**. Then an S_N2 reaction with 2-(Boc-amino)ethyl bromide followed by deprotection of the Boc group produced compound **20**. The final compounds **21**–**31**, **35-40** were obtained by acylation of their corresponding amine precursors with acyl chlorides

or carboxylic acids. The derivatives **32**–**34**, **41-55** were synthesized in a similar fashion.


16a R_1 = H
16b R_1 = CH_3
16c R_1 = Br
16d R_1 = cyclopropyl
16e R_1 = CHF_2
16f R_1 = CF_3
16g R_1 = 1*H*-pyrazol-4-yl

21 R_1 = H, R_2 = acryloyl
22 R_1 = H, R_2 = propionyl
23 R_1 = CH_3, R_2 = acryloyl
24 R_1 = CH_3, R_2 = propionyl
25 R_1 = Br, R_2 = acryloyl
26 R_1 = Cyclopropyl, R_2 = acryloyl
27 R_1 = CHF_2, R_2 = acryloyl
28 R_1 = CHF_2, R_2 = propionyl
29 R_1 = CF_3, R_2 = acryloy

30 R_1 = CF_3, R_2 = propionyl
31 R_1 = 1*H*-pyrazol-4-yl, R_2 = acryloyl
35 R_1 = CHF_2, R_2 = 2-fluoroacetyl
36 R_1 = CHF_2, R_2 = 2-chloroacetyl
37 R_1 = CHF_2, R_2 = but-2-enoyl
38 R_1 = CHF_2, R_2 = 4,4,4-trifluorobut-2-enoyl
39 R_1 = CHF_2, R_2 = 4-(dimethylamino)but-2-enoyl
40 R_1 = CHF_2, R_2 = but-2-ynoyl

Scheme 1. Synthesis of indolylindazole derivatives: (a) TIPSCl, imidazole, DMF, r.t., 1 h; (b) (Boc)$_2$O, Et$_3$N, DMAP, dioxane, r.t., 1 h; (c) LDA, triisopropyl borate, THF, -78 °C, 30 min; (d) I$_2$, K$_2$CO$_3$, DMF, r.t., 3 h; (e) (Boc)$_2$O, Et$_3$N, DMAP, dioxane, r.t., 1 h; (f) Cs$_2$CO$_3$, Pd(dppf)Cl$_2$, dioxane/H$_2$O, microwave, 100 °C, 20 min; (g) TBAF, THF, r.t., 2 h; (h) TFA, DCM, r.t., 10 min; (i) 2-(Boc-amino)ethyl bromide, Cs$_2$CO$_3$, DMF, r.t., 4 h; (j) TFA, DCM, r.t., 10 min; (k) acyl chlorides, Na$_2$CO$_3$, DCM/H$_2$O, 0 °C, 20 min. (l) carboxylic acids, HATU, DIEA, DMF, r.t., 2 h.

3. Results and discussion

3.1 Design strategy

It is noticeable that the three inhibitors in Fig. 1, indolylthienopyrazole **4** [26], indolylindazole **5** [27] and indolyltetrahydroindazole **8** [28], showed nanomolar inhibitory activity (**4**, IC$_{50}$ = 10.9 nM; **5**, IC$_{50}$ = 11 nM; **8**, IC$_{50}$ = 4 nM) against ITK, with their binding modes having clear similarities. The crystal structure of compound **4** complexed with ITK is shown in Fig. 2A (PDB code 3V5J), where the indole NH forms hydrogen bonds with the Met438 backbone oxygen, the pyrazole NH bonding to Met438 backbone nitrogen and the pyrazole NH bonds to the backbone oxygen of Glu436. The *O*-alkyl ether side chain of **4** extends into a channel formed by Ile369, Val377 and Cys442. The morpholine group on this side chain reaches out to the solvent, and the nitrogen atom locates in the vicinity of the sulfur atom of Cys442 (4.7 Å). Hence, the *O*-alkyl ether side chain is an appropriate site for modification with different electrophilic warheads to form covalent bonds with Cys442 (Fig. 2B).
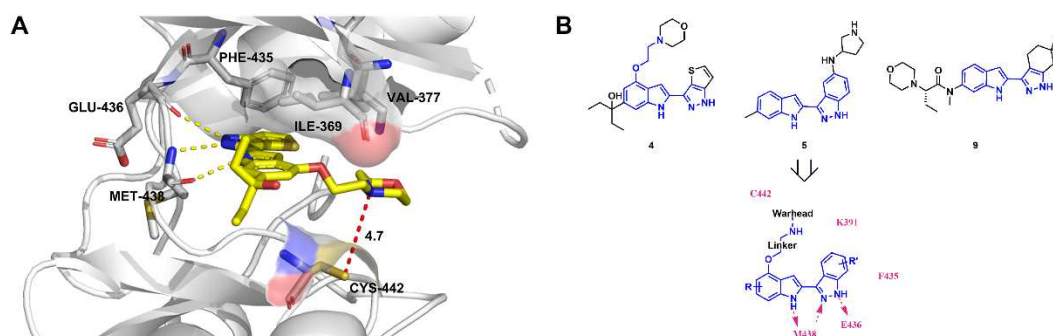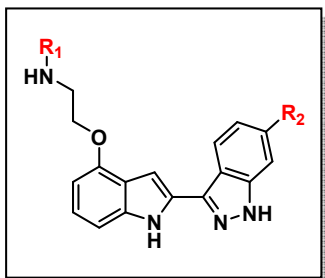

Fig. 2. (A) Cocrystal structure of **4** complexed with the kinase domain of ITK (PDB code 3V5J). The potential hydrogen bonds are depicted by yellow dashed lines. The distance between the sulfur atom of Cys442 and the nitrogen atom of morpholine of **4** (4.7 Å) is shown as a red dashed line. (B) Design strategy for the current series of covalent ITK inhibitors.

3.2 *In vitro* activity against ITK

Inhibitory activities of compounds **20–31** against ITK were evaluated via a well-established homogeneous time-resolved fluorescence (HTRF) assay as shown in Table 1. PRN694 (**9**) was used as the reference compound, which showed an IC_{50} value of 3.2 nM consistent with the data reported in the literature [20].

Table 1. SAR at the indazole moiety.

Compound#	R_1	R_2	IC_{50}^{a} [nM]	Cpd#	R_1	R_2	IC_{50}^{a} [nM]
20a	H	H	102	26	⌇C(=O)CH=CH$_2$	cyclopropyl	111
21	⌇C(=O)CH=CH$_2$	H	64	27	⌇C(=O)CH=CH$_2$	CHF$_2$	5.6
22	⌇C(=O)CH$_2$CH$_3$	H	552	28	⌇C(=O)CH$_2$CH$_3$	CHF$_2$	162
23	⌇C(=O)CH=CH$_2$	CH$_3$	23	29	⌇C(=O)CH=CH$_2$	CF$_3$	156
24	⌇C(=O)CH$_2$CH$_3$	CH$_3$	428	30	⌇C(=O)CH$_2$CH$_3$	CF$_3$	2001
25	⌇C(=O)CH=CH$_2$	Br	40	31	⌇C(=O)CH=CH$_2$	pyrazolyl	6.1

[a] The values are the mean of two independent experiments.

As shown in Table 1, noncovalent compound **20a** inhibited ITK with moderate activity (IC_{50} = 102 nM). It was docked into the ATP-binding site of ITK as depicted in Fig. 3A. As expected, compound **20a** was able to bind with ITK in a similar way to compound **4**, and conserved hydrogen bonds were observed between **20a** and the hinge region of ITK. The amino group located within a reasonable distance (4.1 Å) from the sulfur atom of Cys442 could be potentially targeted with an electrophilic warhead to form a covalent bond. Then a mild acrylamide reactive group was introduced and the resulting compound **21** showed improved ITK inhibitory activity (IC_{50} = 64 nM). A reversible analog **22** bearing a propionamide group was also synthesized, which showed 8-fold lower inhibitory activity compared to **21**.
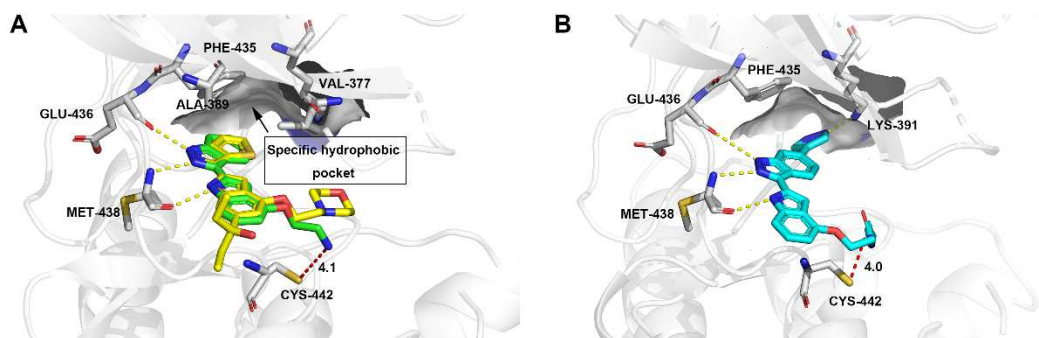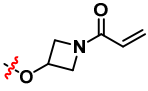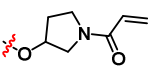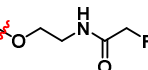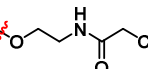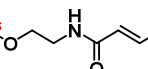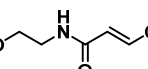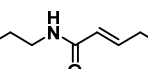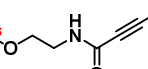
Fig. 3. Docking results for **20a** and **31** in the ATP-binding site of ITK. (A) Overlay of **20a** (carbon atoms in green) and the lead compound **4** (carbon atoms in yellow) bound in the ATP-binding pocket of ITK (PDB code 3V5J). The distance between the nitrogen atom in the *O*-alkyl ether side chain of **20a** and the sulfur atom in Cys442 (4.1 Å) is shown as a red dashed line. (B) Docking result from **31** (carbon atoms in blue) within the ATP-binding pocket of ITK. The distance between the β-carbon in the acylamide group of **31** and the sulfur in Cys442 (4.0 Å) is shown as a red dashed line.

A specific hydrophobic pocket was formed by the side chains of Phe435, Lys391, Val377 and Ala389, as showed in Fig. 3A, which was not occupied by compounds **4** and **20a**. Introduction of substituents through the C6-position of the indazole moiety to occupy this hydrophobic pocket might improve inhibitory activity against ITK. Introduction of a methyl group resulted in a moderate improvement in activity (**23** vs **21**, **24** vs **22**), while Br or a cyclopropyl group (**25**, **26**) did not improve the potency. Fluorinated methyl groups were also introduced at this position. The difluoromethyl group (**27**) exhibited significant potency improvement (IC$_{50}$ = 5.6 nM) compared to **21**, and the reversible analog **28** also showed an over 3-fold higher potency than **22**. However, the trifluoromethyl group (**29**, **30**) exhibited a much-reduced potency likely due to the bulky size of the CF$_3$ group. Compound **31** bearing a pyrazolyl substituent (IC$_{50}$ = 6.1 nM) showed equal potency to **27** possibly attributed to a face-to-face π-π stacking interaction between the pyrazolyl group and the side chain of the gatekeeper Phe435 as well as a hydrogen bond between the pyrazolyl NH and Lys391 (Fig. 3B).

Table 2. SAR of the linker and electrophilic warhead.
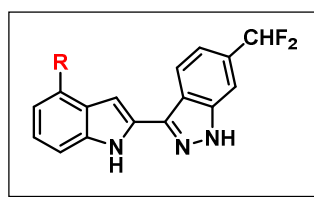
Compound#	R	IC$_{50}$[a] [nM]		Ratio of activities
		ITK	BTK	[BTK/ITK]
27		5.6	25	[4.5×]
32		11	45	[4.1×]

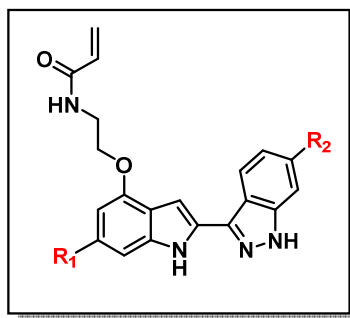| #	Structure			
33		58	71	[1.2×]
34		226	1339	[5.9×]
35		915	NT	NT
36		9	8.9	[1×]
37		84	907	[10.8×]
38		31	15	[0.5×]
39		286	1000	[3.5×]
40		90	340	[3.8×]

[a] The values are the mean of two independent experiments.

With the difluoromethyl group substituted to the indazole fragment, modifications of the *O*-alkyl ether side chain were explored. Compound **32** showed 2-fold reduction in potency. A rigid four- (**33**) or five-membered ring (**34**) resulted in significantly reduced potency. The linear alkyl-chain seems flexible enough to facilitate the warhead reaching Cys442. Next, a panel of electrophilic warheads (**35–40**) was examined, and none of them showed higher activity and selectivity than **27**, except for compound **37**, which showed an 11-fold selectivity over BTK but remarkably decreased activity against ITK.
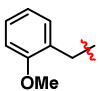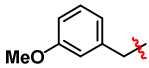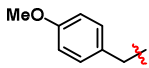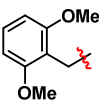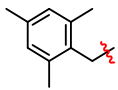
To improve the selectivity of the current series of ITK inhibitors, the residues around the ATP-binding pocket were examined. Two phenylalanine residues (the "gatekeeper" Phe435 and Phe437) are found nearby, which is a relatively rare arrangement in the whole human kinome. It was reported that the π-π interaction between Phe437 and a substituent of inhibitor could improve the selectivity of ITK inhibitors over LCK and Aurora A kinases [29, 30]. We hypothesized that the introduction of an aryl group at the 5-position of the indole moiety in our inhibitors would also benefit from this π-π interaction to gain selectivity improvement. As shown in Table 3, an increased selectivity over BTK was indeed observed in compounds **41** to **43**; especially, the IC_{50} value of **43** was 4 nM with a 33-fold selectivity over BTK. The tetrahydro-2*H*-pyran-4-yl and but-3-yn-1-yl substituents (**44**, **45**) were also tolerated for potency, but the selectivity was not as good as **43**, and the 2-(methylsulfonyl)ethyl substitution group (**46**) yielded a decreased potency for ITK.

Table 3. SAR at the indole moiety.

Compound#	R₁	R₂	IC₅₀ᵃ [nM]		Ratio of activities
			ITK	BTK	[BTK/ITK]
41	Ph₂C(OH)–	CHF_2	25	676	[27×]
42	PhCH(OH)–	CHF_2	3.6	34	[9.4×]
43	PhCH<	CHF_2	4.0	133	[33×]
44	Ph–CH(O-tetrahydropyran)–	CHF_2	6.2	24	[3.9×]
45	Ph–CH(O-butynyl)–	CHF_2	8.5	91	[11×]
46	Ph–CH(OCH₂CH₂SO₂Me)–	CHF_2	65	70	[1.1×]
47	3-Cl-C₆H₄-CH₂–	CHF_2	78	287	[3.7×]
48	3-F₃C-C₆H₄-CH₂–	CHF_2	58	256	[4.4×]
49	3-Me-C₆H₄-CH₂–	CHF_2	34	235	[6.9×]

50		CHF$_2$	32	187	[5.8×]
51		CHF$_2$	9.0	138	[15×]
52		CHF$_2$	5.0	79	[16×]
53		CHF$_2$	25	331	[13×]
54		CHF$_2$	62	445	[7.2×]
55			5.8	186	[32×]

[a] The values are the mean of two independent experiments.

To gain insight into the protein-ligand interactions, compound **43** was docked into the ATP-binding site of ITK and BTK. It showed that compound **43** formed three hydrogen bonds with the hinge region of ITK as compound **4** did (Fig. 4A). It is noticeable that the benzyl group of **43** is approximately perpendicular to the phenyl ring of the Phe473 residue. This kind of edge-to-face arrangement of aromatic rings increases the stability of the complex and is frequently found in chemical and biological systems [31, 32]. However, a similar interaction was not observed between **43** and Tyr476 in BTK (Fig. 4B), which may explain the improved selectivity of **43** favoring ITK over BTK.
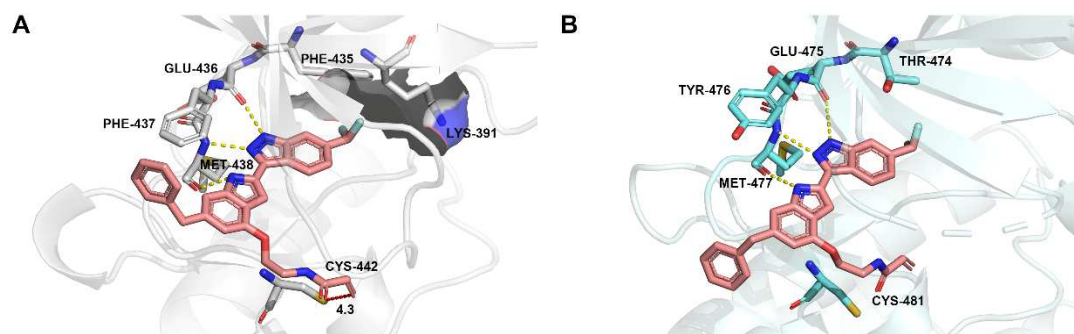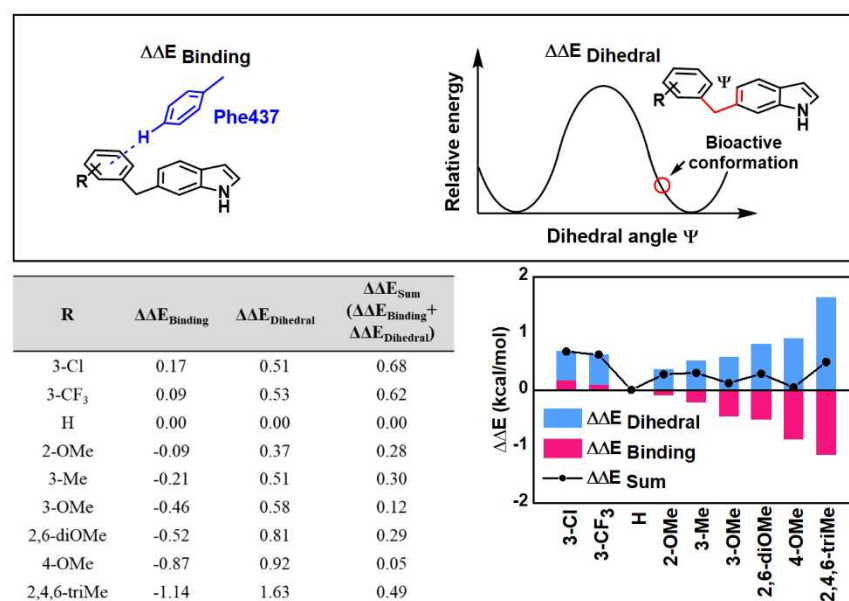

Fig. 4. Docking results for **43** (carbon atoms in pink) in the ATP-binding site of ITK and BTK. (A) **43** docked into the ATP-binding pocket of ITK (PDB code 3V5J). (B) **43** docked into the ATP-binding pocket of BTK (PDB code 3GEN).

It was reported that a change of substituents on the aryl ring may affect the edge-to-face interaction [33].

Introduction of electron-withdrawing groups such as Cl (**47**) and CF_3 (**48**) yielded inhibitors with weaker potency. And the electron-donating substituents such as MeO or Me group (**49–54**) did not substantially improve either the potency or the selectivity. Since the dihedral torsion angle between the substituted benzyl group, which extends into the solvent region and the indole fragment may also play an important role in the activities of inhibitors [34], a computational study was employed to explore the relationship between the substituents and the ITK inhibitory activity. The binding energy of the π-π interaction with Phe437 and the relative energy of the dihedral torsion angle between the substituted benzyl and the indole fragment were calculated. The binding energy ($-\Delta\Delta E_{Binding}$) improved with the change of electron-withdrawing to electron-donating substituents, ranging from 0.17 kcal/mol (3-Cl) to -1.14 kcal/mol (2,4,6-triMe) as shown in Fig. 5, following the order 3-Cl < 3-CF_3 < H < 2-OMe < 3-Me < 3-OMe < 2,6-diOMe < 4-OMe < 2,4,6-triMe. Benzyl groups with either electron-withdrawing or donating substituents showed higher rotational energy barriers ($\Delta E_{Dihedral}$) than the unsubstituted benzyl group. Although neither the π-π interaction binding energy ($\Delta\Delta E_{Binding}$) nor the relative energy of the dihedral torsion angle ($\Delta\Delta E_{Dihedral}$) alone can explain the observed trend for the inhibitory activity of the compounds, the sum of these two types of energies ($\Delta\Delta E_{Sum}$) can shed some light on the matter. The $\Delta\Delta E_{Sum}$ of the benzyl substituted indoles followed the order of 3-Cl < 3-CF_3 < 2,4,6-triMe < 3-Me < 2,6-diOMe < 2-OMe < 3-OMe < 4-OMe < H, which reasonably reflects the order of the inhibitor potency. Overall, the unsubstituted benzyl group was preferred at this substitution point. Compound **55** with a pyrazolyl group at the indazole fragment also presented an IC_{50} of 5.8 nM and a 32-fold selectivity over BTK. Therefore, compounds **43** and **55** were chosen for further evaluation.

Fig. 5. Calculated energies of edge-to-face aromatic interactions and rotational energy barriers[a].

R	$\Delta\Delta E_{Binding}$	$\Delta\Delta E_{Dihedral}$	$\Delta\Delta E_{Sum}$ ($\Delta\Delta E_{Binding}$ + $\Delta\Delta E_{Dihedral}$)
3-Cl	0.17	0.51	0.68
3-CF_3	0.09	0.53	0.62
H	0.00	0.00	0.00
2-OMe	-0.09	0.37	0.28
3-Me	-0.21	0.51	0.30
3-OMe	-0.46	0.58	0.12
2,6-diOMe	-0.52	0.81	0.29
4-OMe	-0.87	0.92	0.05
2,4,6-triMe	-1.14	1.63	0.49

[a] Interaction energies were calculated with the BSSE correction. The relative interaction energies in water were obtained using PCM. The conformation optimization and relative energies were performed using M06-2X-D3 methods. Energies are expressed in kilocalories per mole. The $\Delta\Delta E$ values in the table are values relative to the unsubstituted benzyl group.

3.3 Evidences for covalent binding and kinectic properties of selected compounds

The alkynyl compound **45**, a close analog of **43**, was used as a probe to label and visualize ITK after a

Cu(I)-catalyzed click reaction with BODIPY-N$_3$. The recombinant ITK was successfully labeled and observed under a fluorescence scan (Fig. 6A), suggesting that a covalent bond was formed between **45** and ITK. In competition experiments, labeling of ITK by probe **45** was completely blocked by pretreatment of ITK with compounds **43**, **55** or a known covalent ITK inhibitor **9** (Fig. 6B), suggesting that **43** and **55** irreversibly bind with ITK and they engage Cys442 in ITK in the same way as compound **9**. In contrast, labeling ITK with **45** was not blocked by the reversible inhibitor BMS509744 (**1**).
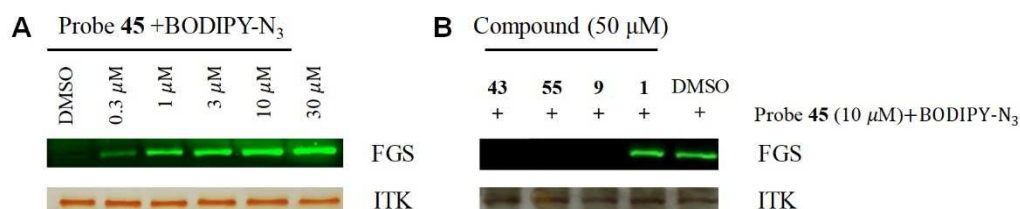
Fig. 6. (A) Labeling ITK with the fluorescent probe precursor **45**. (B) Compound **43** and **55** blocked the labeling of ITK with the fluorescent probe, while BMS509744 (**1**) did not.

We also performed a time-dependent inhibition assay to probe the possibility of irreversible covalent binding between ITK and inhibitors. The activity of ITK was gradually diminished with a prolonged incubation time between ITK and irreversible inhibitors **43** and **55**, whereas the negative control compound - reversible inhibitor **1** did not show such a trend (Fig. 7).
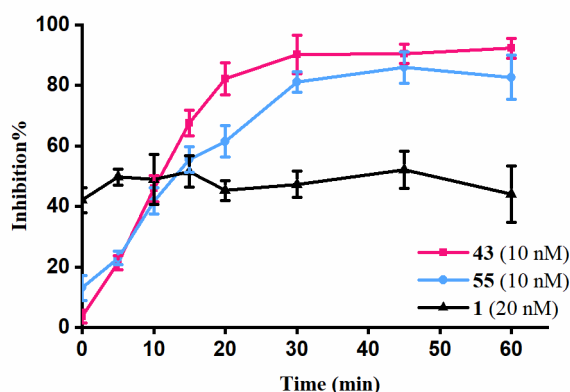
Fig. 7. Time-dependent inhibition curves for compounds **43** and **55**.

To characterize the roles of inhibitor binding affinity and chemical reactivity in overall potency, the kinetic parameters K_i and k_{inact} of the selected compounds were evaluated (Table 4). Compounds **43** and **55** exhibited higher binding affinity and a faster inactivation rate compared to **21**. It suggested that modification of the inhibitor scaffold not only improved the reversible binding affinity but also influenced the chemical reactivity.

Table 4. Kinetics Study [a]

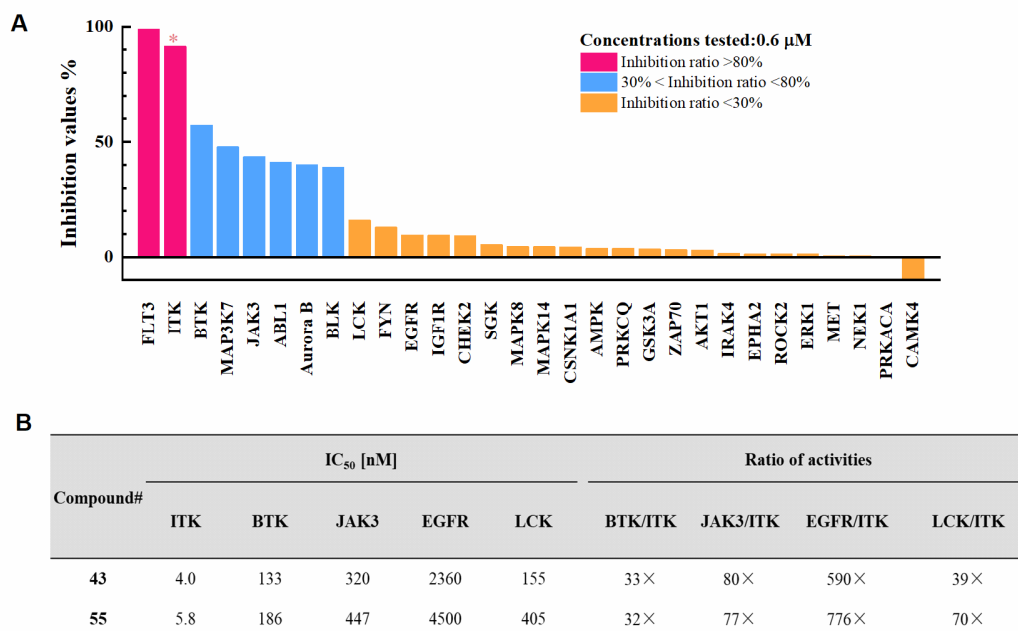| Compound#	K_i (nM)	k_{inact} (min^{-1})	k_{inact} / K_i (10^5 M^{-1} s^{-1})
21	110	0.033	0.05
43	13	0.079	1.0
55	20	0.085	0.71

[a] Kinetic parameters were measured with HTRF KinEASE assays.

3.4 Kinase profiling

The selectivity of compound **43** was profiled against a panel of kinases including representatives of major

subfamilies of kinases and those kinases that directly participate in the TCR pathway. At 0.6 μM, compound **43** was inactive against the majority of kinases tested and showed moderate activity against BTK, MAP3K7, JAK3, ABL1, Aurora B and BLK but potently inhibited FLT3 (Fig. 8A). FLT3 is mainly expressed in hematopoietic cells, but not expressed or expressed at a low level in mature T-cell leukemia cells, such as Jurkat and Molt-4 cells. Moreover, FLT3 does not have a cysteine at the same position as Cys442 in ITK, so the binding of compound **43** and FLT3 is more likely to be noncovalent.

Next, the IC$_{50}$ values for **43** and **55** were determined against BTK, JAK3 and EGFR, which share a cysteine residue at the same position as Cys442 in ITK, and LCK, an SRC kinase upstream of ITK in the TCR pathway (Fig. 8B). Both compound **43** and **55** exhibited an over 30-fold selectivity against those four kinases.


Compound#	IC$_{50}$ [nM]					Ratio of activities			
	ITK	BTK	JAK3	EGFR	LCK	BTK/ITK	JAK3/ITK	EGFR/ITK	LCK/ITK
43	4.0	133	320	2360	155	33×	80×	590×	39×
55	5.8	186	447	4500	405	32×	77×	776×	70×

Fig. 8. (A) Selectivity of compounds **43** against a panel of 30 kinases. (B) Selectivity of compounds **43** and **55** against ITK, BTK, JAK3, EGFR and LCK.

3.5 TCR signaling pathway was blocked by **43** and **55** in T cells

ITK plays an important role in the TCR signaling pathway through phosphorylation of Plcγ1 at the Tyr783 site. Reduced activation of mitogen-activated (MAP) kinases ERK1/2 was observed in the absence of ITK. Jurkat cells were treated with inhibitor **43** or **55** at different concentrations, and then stimulated with anti-CD3/CD28 dynabeads. It was found that phosphorylation of Plcγ1 was completely inhibited at a concentration of 0.3 μM (**43**, EC$_{50}$ = 119 nM; **55**, EC$_{50}$ = 133 nM; Fig. 9A, 10B). Compounds **43** and **55** also inhibited the phosphorylation of ERK1/2 in Jurkat cells, indicating that the activity of ITK is critical in the downstream TCR signaling pathway. In H9 cells, phosphorylation of Plcγ1 was also found to be completely inhibited by **43** and **55** but was not completely inhibited by the reversible inhibitor BMS509744 (**1**) at the same concentration (Fig. 9D).

Next, washout experiments were conducted to confirm the irreversible inhibition of ITK by compounds **43** and **55** in living cells. Jurkat cells were treated with compounds **43**, **55**, **9** (PRN694) and reversible inhibitor **1** (BMS509744) respectively. Covalent inhibitors **43**, **55** and **9** maintained their inhibitory effects in cells even after extensive washing with PBS buffer, whereas Plcγ1 phosphorylation levels were largely restored in cells treated with the reversible inhibitor **1** after removal of the compound (Fig. 9E, 9F).
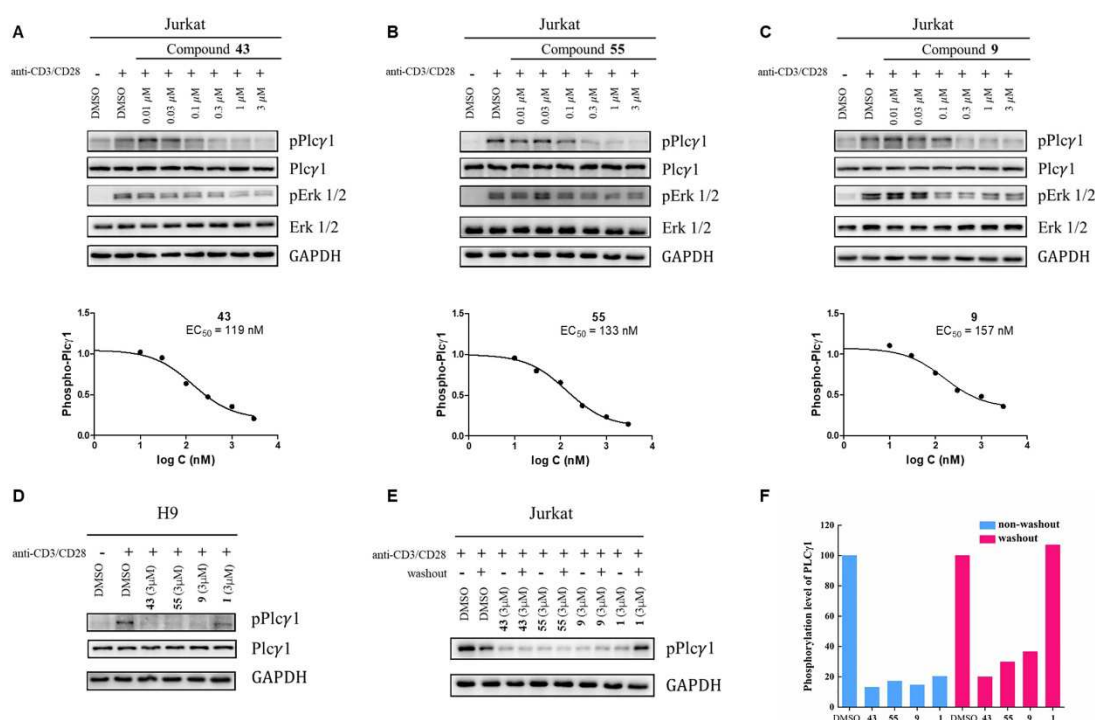
Fig. 9. Compounds **43** and **55** inhibited ITK phosphorylation activity in live Jurkat cells (A, B) and H9 cells (D). Washout experiments with irreversible inhibitors **43**, **55**, **9** and the reversible inhibitor **1** (E, F).

In sharp contrast, compounds **43** and **55** showed almost no inhibitory effect on the phosphorylation of PLCγ2 which is a direct physiological substrate of BTK in Ramos cells, a B cell line that expresses BTK but not ITK. This suggested that **43** and **55** had excellent selectivity against BTK in living cells (Fig. 10).
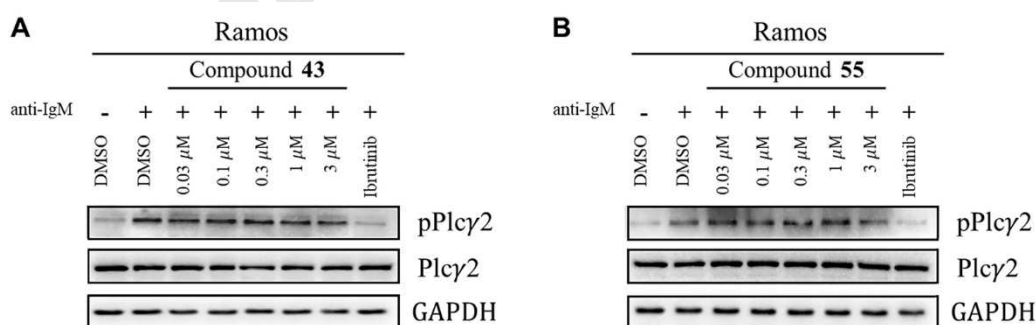
Fig. 10. Compounds **43** (A) and **55** (B) did not inhibit phosphorylation of the BTK substrate in Ramos cells.

3.6 Antiproliferative assay

The effects of **43** and **55** on the growth of leukemia cell lines were evaluated via an ATP luminescence assay. The antiproliferative activities of these two compounds against three T-ALL cell lines (Jurkat, MOLT-4 and CCRF-CEM cells) and a cutaneous T-cell lymphoma cell line (H9) were examined. It was found that **43** and **55** both inhibited growth for these cancer cell lines at low micromolar levels and had weaker inhibitory effects against HEK 293T cells (Table 5). These results suggested that inhibition TCR signaling may not directly induce potent cytotoxicity to T cells [20, 29]. Further study of mechanisms of action for this series of novel covalent ITK

inhibitors in T cells is ongoing in our laboratory.

Table 5. Antiproliferative activities of **43** and **55** in T cells and HEK 293T cells.

Compound#	GI$_{50}$ (μM)				
	Jurkat	**Molt-4**	**CCRF-CEM**	**H9**	**HEK 293T**
43	5.1	3.7	3.4	5.4	19
55	2.8	1.4	0.9	2.0	15

3.7 Pharmacokinetic property evaluation.

In vivo pharmacokinetic (PK) properties of compound **43** were examined in mice intravenously (Table 6). Compound **43** exhibited a short half-life of 0.62 h, high clearance rate (34.4 mL/min/kg), and small distribution volume that means that the compound likely remains in the circulatory system. It is noteworthy that covalent inhibitors do not need to meet classic ADME parameters to be used *in vivo* as is the case for reversible inhibitors, and the relatively rapid clearance rate may lead to a lower propensity for off-target related adverse effects [35].

Table 6. Pharmacokinetic properties of compound **43** in ICR mice

iv (2 mg/kg)	
T$_{1/2}$ (hr)	0.62 ± 0.05
AUC$_{0-t}$ (ng·hr/mL)	974 ± 115.1
AUC$_{0-\infty}$ (ng·hr/mL)	976 ± 113.9
Vz(L/kg)	1.85 ± 0.34
CL(ml/min/kg)	34.4 ± 3.92
Vd$_{ss}$(L/kg)	1.27 ± 0.17
MRT$_{last}$ (hr)	0.59 ± 0.01

4. Conclusions

In summary, we have designed and synthesized a novel series of potent and selective covalent inhibitors for ITK. Structure-activity relationships and computational studies provided insight into the interactions between the kinase and inhibitors to facilitate the optimization process. Functional assays revealed that compounds **43** and **55** could potently inhibit the phosphorylation activity of ITK on downstream substrates and showed excellent selectivity against BTK in live cells. These two compounds may serve as valuable covalent chemical probes for the exploration of the roles of ITK in disease relevant biological systems.

5. Experimental

5.1 Chemistry

All commercially available reagents and solvents were used as received. Reactions using air- or moisture-sensitive reagents were performed under an atmosphere of nitrogen. Reaction progress was monitored by TLC and/or HPLC. Flash column chromatography was conducted using silica gel. NMR spectra were measured using Bruker 400 or 500 MHz spectrometers, and chemical shifts are reported in units of ppm downfield from TMS using residual nondeuterated solvent as internal standards (CHCl$_3$, 7.26 ppm; DMSO, 2.50 ppm; MeOH, 3.31 ppm, (CH$_3$)CO, 2.05 ppm). In the NMR tabulation, s indicates singlet, d indicates doublet, t indicates triplet, q indicates quartet, m indicates multiplet and br indicates broad peak. The purities of all final compounds were determined by HPLC to be above 95%.

*5.1.1 Tert-butyl 4-((triisopropylsilyl)oxy)-1H-indole-1-carboxylate (**14**)*

Compound **13** (1.3 g, 10 mmol) was dissolved in DMF (10.0 mL), and the solution was added to imidazole (1.0 g, 15 mmol) and triisopropylsilyl chloride (2.3 g, 12 mmol), followed by stirring at room temperature for 5 h. The reaction mixture was quenched with water and extracted with ethyl acetate. The organic layer was washed with brine and dried over anhydrous sodium sulfate. The solvent was evaporated under reduced pressure to give a crude product which was dissolved in dioxane (20 mL) followed by the addition of Et_3N (3.0 mL, 22 mmol), $(Boc)_2O$ (2.5 mL, 11 mmol) and DMAP (1.2 mg, 0.10 mmol). The reaction mixture was then stirred at room temperature for 1 h. Next, the mixture was diluted with saturated $NaHCO_3$ (aq.) and extracted three times with ethyl acetate. The organic layer was washed with brine and dried over anhydrous sodium sulfate. The solvent was evaporated under reduced pressure and the residue was purified by flash column chromatography (hexane/ethyl acetate = 20/1) to yield **14** as a yellow oil (3.1 g, 80%). ^{1}H NMR (400 MHz, $CDCl_3$) δ 7.89 (d, J = 8.4 Hz, 1H), 7.59 (d, J = 3.7 Hz, 1H), 7.24 (t, J = 8.1 Hz, 1H), 6.85 – 6.71 (m, 2H), 1.73 (s, 9H), 1.47 – 1.36 (m, 3H), 1.23 (d, J = 7.7 Hz, 18H). ^{13}C NMR (101 MHz, $CDCl_3$) δ 149.87, 149.29, 136.99, 125.02, 124.31, 123.66, 111.52, 108.67, 104.85, 83.38, 28.18, 18.11, 13.00. HRMS (ESI) m/z calcd. for $C_{22}H_{36}NO_3Si$ [M+H]$^+$ 390.2459, found 390.2461.

*5.1.2 (1-(Tert-butoxycarbonyl)-4-((triisopropylsilyl)oxy)-1H-indol-2-yl)boronic acid (**15**)*

To a solution of compound **14** (3.1 g, 8.0 mmol) and triisopropyl borate (6.0 g, 32 mmol) in THF (40 mL) at -78 °C was dropwise added LDA (2.0 M in THF, 32 mL, 32 mmol). The mixture was stirred at -78 °C for 1 h, then quenched with saturated NH_4Cl (aq.) (40 mL) and stirred for 15 min without cooling. Next, the mixture was extracted three times with ethyl acetate, and the organic layer was washed with brine and dried over anhydrous sodium sulfate. The solvent was evaporated under reduced pressure to give a crude product **15** (2.4 g, 70%) which was immediately used for the next step without further purification.

*5.1.3 Tert-butyl 3-iodo-1H-indazole-1-carboxylate (**17a**)*

To a stirred solution of indazole **16** (1.2 g, 10 mmol) in DMF (10 mL) was added potassium carbonate (1.0 g, 20 mmol) and iodine (3.0 g, 12 mmol). The mixture was then stirred at room temperature overnight. Next, the reaction mixture was poured into 100 mL aq. $NaHSO_3$ (10%) and extracted three times with ethyl acetate. The organic layer was washed with brine and dried over anhydrous sodium sulfate. The solvent was evaporated under reduced pressure to give a crude product which was immediately dissolved in dioxane (20 mL) followed by the addition of Et_3N (3.0 mL, 22 mmol), $(Boc)_2O$ (2.5 mL, 11 mmol) and DMAP (0.0012 g, 0.1 mmol). The reaction mixture was stirred at room temperature for 1 h, and then diluted with saturated $NaHCO_3$ (aq) and extracted with ethyl acetate. The organic layer was washed with brine and dried over anhydrous sodium sulfate. The solvent was evaporated under reduced pressure and the residue was purified by flash column chromatography (hexane/ethyl acetate=10/1) to yield **17a** as a yellow solid (2.8 g, 82%). ^{1}H NMR (400 MHz, $CDCl_3$) δ 8.12 (d, J = 8.5 Hz, 1H), 7.60 – 7.56 (m, 1H), 7.49 (dt, J = 8.0, 1.1 Hz, 1H), 7.39 – 7.35 (m, 1H), 1.72 (s, 9H). ^{13}C NMR (101 MHz, $CDCl_3$) δ 148.36, 139.62, 130.19, 129.96, 124.18, 121.97, 114.56, 102.89, 85.49, 28.15. HRMS (ESI) m/z calcd. for $C_{12}H_{14}IN_2O_2$ [M+H]$^+$ 345.0094, found 345.0092.

*5.1.4 Tert-butyl 3-(4-((triisopropylsilyl)oxy)-1H-indol-2-yl)-1H-indazole-1-carboxylate (**18a**)*

A mixture of **15** (0.560 g, 1.28 mmol), **17a** (0.400 g, 1.06 mmol), cesium carbonate (1.68 g, 5.12 mmol) and [1,1'-bis(diphenylphosphino)ferrocene]palladium(II) dichloride (0.026 mg, 0.032 mmol) in dioxane (8.0 mL) and H_2O (2.0 mL) was purged with argon. The reaction was then sealed and heated with stirring under microwave irradiation at 100 °C for 20 min. Next, the reaction mixture was quenched with water and extracted with ethyl acetate. The organic layer was washed with brine and dried over anhydrous sodium sulfate. The solvent was evaporated under reduced pressure and the residue was purified by flash column chromatography (hexane/ethyl acetate = 4/1) to yield **18a** as a yellow solid (0.35 g, 55%). ^{1}H NMR (500 MHz, $CDCl_3$) δ 7.93 (d, J = 8.3 Hz, 1H), 7.64 (d, J = 8.1 Hz, 1H), 7.32 – 7.21 (m, 3H), 7.14 (ddd, J = 7.9, 6.0, 1.7 Hz, 1H), 7.02 (s, 1H), 6.75 (d, J = 7.9 Hz, 1H), 1.37-1.31 (m, 3H), 1.11 (d, J = 7.6 Hz, 18H), 1.06 (s, 9H). ^{13}C NMR (126 MHz, $CDCl_3$) δ 150.03, 149.28,

140.61, 139.23, 129.57, 126.92, 125.65, 123.30, 122.25, 121.12, 120.75, 111.57, 110.04, 109.55, 108.70, 83.34, 27.23, 18.03, 12.88. HRMS (ESI) m/z calcd. for $C_{29}H_{40}N_3O_3Si$ [M+H]$^+$ 506.2833, found 506.2831.

5.1.5 2-(1H-indazol-3-yl)-1H-indol-4-ol (19a)

To compound **18a** (0.35 g, 0.70 mmol) in 5 mL THF at 0 °C was added 0.80 mL TBAF (1 mol/L in THF, 0.80 mmol). The mixture was stirred at room temperature for 1 h, and then quenched with saturated NH$_4$Cl (aq). Next, the mixture was extracted three times with ethyl acetate, and the organic layer was washed with brine and dried over anhydrous sodium sulfate. The solvent was evaporated under reduced pressure to give a crude product which was immediately dissolved in 20% TFA/DCM (10 mL). The reaction was then stirred for 20 min at room temperature. Next, the mixture was carefully neutralized with solid NaHCO$_3$. The solids were filtered off and the solvents were evaporated to give a crude product which was purified by flash column chromatography (hexane/ethyl acetate = 2/1) to yield **19a** as a yellow solid (0.14 g, 81%). ^{1}H NMR (500 MHz, Acetone-*d$_6$*) δ 10.66 (s, 1H), 8.22 (d, *J* = 8.1 Hz, 1H), 7.65 (d, *J* = 8.3 Hz, 1H), 7.46 (ddd, *J* = 8.3, 6.8, 1.0 Hz, 1H), 7.35 (d, *J* = 2.3 Hz, 1H), 7.32 – 7.26 (m, 1H), 7.08 (d, *J* = 8.1 Hz, 1H), 7.00 (t, *J* = 7.8 Hz, 1H), 6.52 (d, *J* = 7.5 Hz, 1H). ^{13}C NMR (126 MHz, Acetone-*d$_6$*) δ 150.66, 141.87, 138.62, 138.41, 130.13, 126.54, 123.13, 121.13, 120.65, 120.41, 119.26, 110.40, 103.66, 103.35, 97.46. HRMS (ESI) m/z calcd. for $C_{15}H_{12}N_3O$ [M+H]$^+$ 250.0975, found 250.0973.

5.1.6 2-((2-(1H-indazol-3-yl)-1H-indol-4-yl)oxy)ethan-1-amine (20a)

To a stirred solution of **19a** (0.12 g, 0.46 mmol) and Cs$_2$CO$_3$ (0.450 g, 1.38 mmol) in DMF (5 mL), *N*-Boc-protected-bromoalkane (0.16 g, 0.69 mmol) was added. The mixture was stirred at room temperature for 1 h, and then quenched with water and extracted with ethyl acetate. Next, the organic layer was washed with brine and dried over anhydrous sodium sulfate. The solvent was evaporated under reduced pressure and the residue was purified by flash column chromatography (DCM/MeOH = 20/1) to obtain **20a** as a brown solid (0.094 g, 70%). ^{1}H NMR (500 MHz, DMSO-*d$_6$*) δ 13.43 (s, 1H), 11.62 (d, *J* = 2.3 Hz, 1H), 8.26 (d, *J* = 8.2 Hz, 1H), 7.62 (d, *J* = 8.4 Hz, 1H), 7.48 – 7.41 (m, 1H), 7.39 (d, *J* = 2.2 Hz, 1H), 7.27 (dd, *J* = 8.1, 6.9 Hz, 1H), 7.10 (d, *J* = 8.1 Hz, 1H), 7.03 (t, *J* = 7.8 Hz, 1H), 6.53 (d, *J* = 7.6 Hz, 1H), 4.33 (t, *J* = 5.1 Hz, 2H), 3.33 (t, *J* = 5.1 Hz, 2H). ^{13}C NMR (126 MHz, DMSO-*d$_6$*) δ 151.71, 141.78, 138.32, 137.93, 130.58, 130.11, 126.85, 122.85, 121.39, 121.14, 120.31, 119.85, 111.07, 105.98, 100.70, 98.25, 64.39. HRMS (ESI) m/z calcd. for $C_{17}H_{17}N_4O$ [M+H]$^+$ 293.1397, found 293.1394.

5.1.7 N-(2-((2-(1H-indazol-3-yl)-1H-indol-4-yl)oxy)ethyl)acrylamide (21)

To **20a** (0.040 g, 0.14 mmol) and sodium carbonate (0.074 g, 0.70 mmol) in 3.0 mL DCM and 2.0 mL H$_2$O at 0 °C was added acyl chloride (0.015 g, 0.17 mmol). The reaction mixture was then stirred for 20 min and quenched with saturated NH$_4$Cl (aq.). Next, the mixture was extracted three times with DCM. The organic layer was washed with brine and dried over anhydrous sodium sulfate. The solvent was evaporated under reduced pressure and the residue was purified by flash column chromatography (hexane/ethyl acetate = 2/1) to obtain **21** as a yellow solid (0.027 g, 56%). ^{1}H NMR (500 MHz, Acetone-*d$_6$*) δ 12.36 (s, 1H), 10.72 (s, 1H), 8.19 (d, *J* = 8.1 Hz, 1H), 7.74 (s, 1H), 7.64 (d, *J* = 8.4 Hz, 1H), 7.52 – 7.41 (m, 1H), 7.29 (t, *J* = 7.6 Hz, 1H), 7.22 (s, 1H), 7.17 (d, *J* = 8.2 Hz, 1H), 7.07 (t, *J* = 7.9 Hz, 1H), 6.58 (d, *J* = 7.6 Hz, 1H), 6.37 (dd, *J* = 17.0, 10.1 Hz, 1H), 6.26 (dd, *J* = 17.0, 2.4 Hz, 1H), 5.59 (dd, *J* = 10.1, 2.4 Hz, 1H), 4.28 (t, *J* = 5.5 Hz, 2H), 3.81 (q, *J* = 5.6 Hz, 2H). ^{13}C NMR (126 MHz, Acetone-*d$_6$*) δ 166.76, 154.25, 143.66, 140.05, 139.93, 133.51, 132.16, 128.33, 126.54, 124.71, 122.91, 122.43, 122.14, 121.85, 112.20, 106.75, 102.34, 99.37, 68.46, 40.69. HRMS (ESI) m/z calcd. for $C_{20}H_{19}N_4O_2$ [M+H]$^+$ 347.1503, found 347.1500.

5.1.8 N-(2-((2-(1H-indazol-3-yl)-1H-indol-4-yl)oxy)ethyl)propionamide (22)

^{1}H NMR (400 MHz, MeOD) δ 8.15 (d, *J* = 8.2 Hz, 1H), 7.60 – 7.52 (m, 1H), 7.48 – 7.39 (m, 1H), 7.30 – 7.22 (m, 1H), 7.17 (d, *J* = 0.8 Hz, 1H), 7.14 – 7.00 (m, 3H), 6.53 (dd, *J* = 7.3, 1.1 Hz, 1H), 4.21 (t, *J* = 5.4 Hz, 3H), 3.69 (t, *J* = 5.4 Hz, 3H), 2.26 (q, *J* = 7.6 Hz, 3H), 1.15 (t, *J* = 7.6 Hz, 4H). ^{13}C NMR (101 MHz, MeOD) δ 176.06,

152.33, 141.68, 138.19, 129.88, 126.47, 122.55, 120.81, 120.48, 120.22, 119.81, 109.92, 104.58, 100.18, 97.53, 66.35, 38.95, 28.78, 9.12. HRMS (ESI) m/z calcd. for $C_{20}H_{20}N_4O_2Na$ [M+Na]$^+$ 371.1478, found 371.1479.

5.1.9 N-(2-((2-(6-methyl-1H-indazol-3-yl)-1H-indol-4-yl)oxy)ethyl)acrylamide (23)

^{1}H NMR (400 MHz, MeOD) δ 8.01 (d, *J* = 8.3 Hz, 1H), 7.33 (s, 1H), 7.15 – 7.02 (m, 4H), 6.54 (dd, *J* = 7.2, 1.2 Hz, 1H), 6.41 – 6.19 (m, 2H), 5.67 (dd, *J* = 9.5, 2.5 Hz, 1H), 4.25 (t, *J* = 5.4 Hz, 2H), 3.78 (t, *J* = 5.4 Hz, 2H), 2.50 (s, 3H). ^{13}C NMR (126 MHz, MeOD) δ 167.12, 152.25, 142.27, 138.21, 138.17, 136.97, 130.59, 129.96, 125.49, 123.06, 122.50, 120.11, 119.79, 118.46, 109.20, 104.61, 100.18, 97.46, 66.26, 39.03, 20.52. HRMS (ESI) m/z calcd. for $C_{21}H_{21}N_4O_2$ [M+H]$^+$ 361.1659, found 361.1660.

5.1.10 N-(2-((2-(6-methyl-1H-indazol-3-yl)-1H-indol-4-yl)oxy)ethyl)propionamide (24)

^{1}H NMR (400 MHz, MeOD) δ 8.02 (d, *J* = 8.3 Hz, 1H), 7.34 (s, 1H), 7.15 – 7.02 (m, 3H), 6.53 (dd, *J* = 7.2, 1.2 Hz, 1H), 4.22 (t, *J* = 5.4 Hz, 2H), 3.70 (t, *J* = 5.4 Hz, 2H), 2.51 (s, 3H), 2.27 (q, *J* = 7.6 Hz, 2H), 1.16 (t, *J* = 7.6 Hz, 3H). ^{13}C NMR (101 MHz, MeOD) δ 176.06, 152.30, 142.29, 138.17, 136.97, 129.97, 123.07, 122.52, 120.08, 119.79, 118.47, 109.21, 104.57, 100.17, 97.48, 66.33, 38.95, 28.78, 20.52, 9.13. HRMS (ESI) m/z calcd. for $C_{21}H_{23}N_4O_2$ [M+H]$^+$ 363.1816, found 363.1819.

5.1.11 N-(2-((2-(6-bromo-1H-indazol-3-yl)-1H-indol-4-yl)oxy)ethyl)acrylamide (25)

^{1}H NMR (400 MHz, MeOD) δ 8.06 (dd, *J* = 8.7, 0.7 Hz, 1H), 7.74 (dd, *J* = 1.7, 0.7 Hz, 1H), 7.35 (dd, *J* = 8.7, 1.6 Hz, 1H), 7.15 (d, *J* = 0.7 Hz, 1H), 7.12 – 7.02 (m, 2H), 6.53 (dd, *J* = 6.8, 1.7 Hz, 1H), 6.40 – 6.20 (m, 2H), 5.67 (dd, *J* = 9.5, 2.6 Hz, 1H), 4.25 (t, *J* = 5.4 Hz, 2H), 3.78 (t, *J* = 5.4 Hz, 2H). ^{13}C NMR (101 MHz, MeOD) δ 167.13, 152.33, 142.41, 138.76, 138.26, 130.60, 129.26, 125.48, 124.17, 122.77, 122.00, 120.56, 119.78, 119.15, 112.77, 104.66, 100.25, 97.82, 66.29, 39.03. HRMS (ESI) m/z calcd. for $C_{20}H_{17}BrN_4O_2Na$ [M+Na]$^+$ 447.0427, found 447.0426.

5.1.12 N-(2-((2-(6-cyclopropyl-1H-indazol-3-yl)-1H-indol-4-yl)oxy)ethyl)acrylamide (26)

^{1}H NMR (400 MHz, Acetone-*d₆*) δ 12.19 (s, 1H), 10.68 (s, 1H), 8.03 (dd, *J* = 8.5, 0.8 Hz, 1H), 7.74 (s, 1H), 7.31 (s, 1H), 7.22 – 7.11 (m, 2H), 7.10 – 7.00 (m, 2H), 6.57 (dd, *J* = 7.7, 0.7 Hz, 1H), 6.45 – 6.19 (m, 2H), 5.59 (dd, *J* = 10.0, 2.4 Hz, 1H), 4.27 (t, *J* = 5.5 Hz, 2H), 3.81 (q, *J* = 5.6 Hz, 2H), 2.14 – 2.07 (m, 1H), 1.09 – 0.96 (m, 2H), 0.86 – 0.71 (m, 2H). ^{13}C NMR (101 MHz, Acetone-*d₆*) δ 165.07, 152.43, 143.18, 142.51, 138.13, 138.08, 131.72, 130.53, 124.81, 122.85, 120.35, 120.07, 120.01, 118.82, 106.36, 104.96, 100.56, 97.47, 66.67, 38.94, 15.49, 9.05. HRMS (ESI) m/z calcd. for $C_{23}H_{23}N_4O_2$ [M+H]$^+$ 387.1816, found 387.1812.

5.1.13 N-(2-((2-(6-(difluoromethyl)-1H-indazol-3-yl)-1H-indol-4-yl)oxy)ethyl)acrylamide (27)

^{1}H NMR (400 MHz, MeOD) δ 8.27 (dd, *J* = 8.5, 0.9 Hz, 1H), 7.75 (s, 1H), 7.46 – 7.38 (m, 1H), 7.20 (d, *J* = 0.7 Hz, 1H), 7.13 – 7.03 (m, 2H), 6.86 (t, *J* = 60.0 Hz, 1H), 6.54 (dd, *J* = 7.1, 1.4 Hz, 1H), 6.41 – 6.22 (m, 2H), 5.67 (dd, *J* = 9.5, 2.5 Hz, 1H), 4.26 (t, *J* = 5.4 Hz, 2H), 3.79 (t, *J* = 5.4 Hz, 2H). ^{13}C NMR (101 MHz, MeOD) δ 167.13, 152.33, 140.99, 138.65, 138.26, 133.30 (t, *J* = 22.2 Hz), 130.61, 129.44, 125.48, 122.74, 121.37, 119.80, 117.70 (t, *J* = 5.2 Hz), 115.21 (t, *J* = 237.4 Hz), 107.89 (t, *J* = 7.5 Hz), 104.67, 100.26, 97.78, 66.30, 39.03. ^{19}F NMR (376 MHz, MeOD) δ -110.70. HRMS (ESI) m/z calcd. for $C_{21}H_{18}F_2N_4O_2Na$ [M+Na]$^+$ 419.1290, found 419.1291.

5.1.14 N-(2-((2-(6-(difluoromethyl)-1H-indazol-3-yl)-1H-indol-4-yl)oxy)ethyl)propionamide (28)

^{1}H NMR (400 MHz, MeOD) δ 8.31 – 8.22 (m, 1H), 7.74 (s, 1H), 7.40 (dd, *J* = 8.5, 1.3 Hz, 1H), 7.20 (d, *J* = 0.8 Hz, 1H), 7.12 – 7.03 (m, 2H), 6.84 (t, *J* = 56.3 Hz, 1H), 6.52 (dd, *J* = 7.1, 1.4 Hz, 1H), 4.20 (t, *J* = 5.5 Hz, 2H), 3.69 (t, *J* = 5.4 Hz, 2H), 2.26 (q, *J* = 7.6 Hz, 2H), 1.14 (t, *J* = 7.6 Hz, 3H). ^{13}C NMR (126 MHz, MeOD) δ 176.07, 152.37, 140.97, 138.63, 138.23, 133.28 (t, *J* = 22.1 Hz), 129.41, 122.75, 121.35, 119.75, 117.69 (t, *J* = 5.1 Hz), 115.21 (t, *J* = 237.1 Hz), 107.91 (t, *J* = 7.5 Hz), 104.60, 100.10, 97.79, 66.30, 38.94, 28.78, 9.14. HRMS (ESI) m/z calcd. for $C_{21}H_{21}F_2N_4O_2$ [M+H]$^+$ 399.1627, found 399.1624.

5.1.15 N-(2-((2-(6-(trifluoromethyl)-1H-indazol-3-yl)-1H-indol-4-yl)oxy)ethyl)acrylamide (29)

¹H NMR (400 MHz, DMSO-*d₆*) δ 13.78 (s, 1H), 11.70 (s, 1H), 8.38 – 8.46 (m, 2H), 8.00 (s, 1H), 7.54 (dd, *J* = 8.6, 1.5 Hz, 1H), 7.16 (d, *J* = 2.4 Hz, 1H), 7.13 – 6.99 (m, 2H), 6.56 (d, *J* = 7.4 Hz, 1H), 6.29 – 6.37 (m, 1H), 6.12 – 6.18 (m, 1H), 5.62 (dd, *J* = 10.1, 2.3 Hz, 1H), 4.19 (t, *J* = 5.7 Hz, 2H), 3.65 (dd, *J* = 5.8, 2.0 Hz, 2H). ¹³C NMR (101 MHz, DMSO-*d₆*) δ 165.42, 152.37, 140.68, 138.52, 132.18, 129.67, 127.83, 127.53, 127.22, 127.22, 126.41, 125.75, 123.70, 123.36, 122.65, 122.11, 119.82, 117.45, 108.93, 105.69, 101.20, 98.13, 66.90, 38.96. HRMS (ESI) m/z calcd. for $C_{21}H_{18}F_3N_4O_2$ [M+H]⁺ 415.1376, found 415.1379.

*5.1.16 N-(2-((2-(6-(trifluoromethyl)-1H-indazol-3-yl)-1H-indol-4-yl)oxy)ethyl)propionamide (**30**)*

¹H NMR (400 MHz, DMSO-*d₆*) δ 13.79 (s, 1H), 11.70 (s, 1H), 8.41 (d, *J* = 8.5 Hz, 1H), 8.09 (t, *J* = 5.7 Hz, 1H), 8.00 (s, 1H), 7.54 (dd, *J* = 8.6, 1.5 Hz, 1H), 7.17 (d, *J* = 2.1 Hz, 1H), 7.11 – 7.03 (m, 2H), 6.56 (dd, *J* = 7.5, 1.0 Hz, 1H), 4.15 (t, *J* = 5.8 Hz, 2H), 3.56 (q, *J* = 5.8 Hz, 2H), 2.16 (q, *J* = 7.6 Hz, 2H), 1.03 (t, *J* = 7.6 Hz, 3H). ¹³C NMR (101 MHz, DMSO-*d₆*) δ 173.71, 152.44, 140.67, 138.52, 129.63, 127.55, 127.23, 126.92, 126.41, 123.70, 123.36, 122.66, 122.11, 119.82, 117.47, 108.94, 105.62, 101.11, 98.17, 66.97, 38.80, 28.94, 10.37. HRMS (ESI) m/z calcd. for $C_{21}H_{20}F_3N_4O_2$ [M+H]⁺ 417.1533, found 417.1530.

*5.1.17 N-(2-((2-(6-(1H-pyrazol-4-yl)-1H-indazol-3-yl)-1H-indol-4-yl)oxy)ethyl)acrylamide (**31**)*

¹H NMR (400 MHz, MeOD) δ 8.14 (d, *J* = 8.5 Hz, 1H), 8.07 (s, 2H), 7.72 (s, 1H), 7.52 (dd, *J* = 8.5, 1.4 Hz, 1H), 7.17 (s, 1H), 7.13 – 7.02 (m, 2H), 6.55 (dd, *J* = 7.2, 1.2 Hz, 1H), 6.40 – 6.24 (m, 2H), 5.68 (dd, *J* = 9.5, 2.5 Hz, 1H), 4.27 (t, *J* = 5.4 Hz, 2H), 3.80 (t, *J* = 5.4 Hz, 2H). ¹³C NMR (126 MHz, MeOD) δ 167.14, 152.28, 145.21, 142.42, 138.44, 138.21, 136.60, 131.63, 130.59, 129.82, 125.52, 122.58, 122.36, 120.95, 119.86, 119.79, 118.96, 105.64, 104.64, 100.19, 97.56, 66.25, 39.04. HRMS (ESI) m/z calcd. for $C_{23}H_{20}N_6O_2Na$ [M+Na]⁺ 435.1540, found 435.1540.

*5.1.18 N-(1-(((2-(6-(difluoromethyl)-1H-indazol-3-yl)-1H-indol-4-yl)oxy)methyl)cyclopropyl)acrylamide (**32**)*

¹H NMR (400 MHz, MeOD) δ 8.27 (d, *J* = 8.5 Hz, 1H), 7.76 (s, 1H), 7.42 (d, *J* = 8.1 Hz, 1H), 7.18 (d, *J* = 0.8 Hz, 1H), 7.11 – 6.99 (m, 2H), 6.86 (t, *J* = 56.2 Hz, 1H), 6.49 (dd, *J* = 7.4, 1.1 Hz, 1H), 6.28 – 6.19 (m, 2H), 5.64 – 5.60 (m, 1H), 4.24 (s, 2H), 1.08 – 0.95 (m, 4H). ¹³C NMR (101 MHz, MeOD) δ 167.70, 152.69, 141.03, 138.65, 138.27, 133.32 (t, *J* = 7.4, 23.2 Hz), 130.82, 129.36, 125.47, 122.75, 121.32, 119.89, 117.64 (t, *J* = 5.1 Hz), 115.21 (t, *J* = 237.1 Hz), 107.98, 104.58, 100.72, 97.78, 71.71, 32.34, 11.01. ¹⁹F NMR (376 MHz, MeOD) δ -110.73. HRMS (ESI) m/z calcd. for $C_{23}H_{21}F_2N_4O_2$ [M+H]⁺ 423.1627, found 423.1629.

*5.1.19 1-(3-((2-(6-(Difluoromethyl)-1H-indazol-3-yl)-1H-indol-4-yl)oxy)azetidin-1-yl)prop-2-en-1-one (**33**)*

¹H NMR (500 MHz, MeOD) δ 8.28 (d, *J* = 8.4 Hz, 1H), 7.77 (s, 1H), 7.43 (d, *J* = 8.5 Hz, 1H), 7.19 (s, 1H), 7.16 (d, *J* = 8.1 Hz, 1H), 7.08 (t, *J* = 7.9 Hz, 1H), 6.94 (t, *J* = 56.2 Hz, 1H), 6.40 (dd, *J* = 17.0, 10.3 Hz, 1H), 6.33 – 6.26 (m, 2H), 5.77 (dd, *J* = 10.3, 1.9 Hz, 1H), 5.25 (dt, *J* = 6.3, 2.7 Hz, 1H), 4.79 (dd, *J* = 9.6, 6.6 Hz, 1H), 4.56 (dd, *J* = 11.3, 6.5 Hz, 1H), 4.42 (dd, *J* = 9.9, 3.6 Hz, 1H), 4.20 (dd, *J* = 11.3, 3.6 Hz, 1H). ¹³C NMR (126 MHz, MeOD) δ 166.33, 149.84, 140.96, 138.47, 133.30 (t, *J* = 22.3 Hz), 129.91, 126.90, 125.75, 122.58, 121.36, 121.31, 119.64, 117.82 (t, *J* = 5.1 Hz), 115.20 (t, *J* = 237.2 Hz), 107.90 (t, *J* = 7.5 Hz), 105.40, 100.31, 97.37, 65.46, 57.57, 55.18, 48.44. HRMS (ESI) m/z calcd. for $C_{22}H_{19}F_2N_4O_2$ [M+H]⁺ 409.1471, found 409.1475.

*5.1.20 1-(3-((2-(6-(Difluoromethyl)-1H-indazol-3-yl)-1H-indol-4-yl)oxy)pyrrolidin-1-yl)prop-2-en-1-one (**34**)*

¹H NMR (500 MHz, Acetone-*d₆*) δ 12.76 (s, 1H), 10.86 (s, 1H), 8.33 (d, *J* = 8.4 Hz, 1H), 7.89 (s, 1H), 7.47 (d, *J* = 8.4 Hz, 1H), 7.32 – 6.94 (m, 4H), 6.82 – 6.54 (m, 2H), 6.40 – 6.24 (m, 1H), 5.65 (ddd, *J* = 25.7, 10.2, 2.5 Hz, 1H), 5.29 (dt, *J* = 35.3, 3.8 Hz, 1H), 4.10 – 3.69 (m, 5H), 2.51 – 2.19 (m, 2H). ¹³C NMR (126 MHz, Acetone-*d₆*) δ 163.77, 163.75, 150.77 (d, *J* = 9.1 Hz), 141.19, 138.49, 133.02 (td, *J* = 22.2, 2.2 Hz), 130.10 (d, *J* = 9.7 Hz), 129.48, 129.44, 129.32, 126.18, 123.05, 121.60 (d, *J* = 20.5 Hz), 120.79 (d, *J* = 5.4 Hz), 118.11 (q, *J* = 5.3 Hz), 115.41 (t, *J* = 236.7 Hz), 108.54 (q, *J* = 7.1, 6.5 Hz), 105.42, 105.38, 105.31, 102.51 (d, *J* = 8.2 Hz), 97.78 (d, *J* = 6.7 Hz), 77.06, 75.33, 51.74 (d, *J* = 47.9 Hz), 44.51, 43.91, 31.76. HRMS (ESI) m/z calcd. for $C_{23}H_{21}F_2N_4O_2$ [M+H]⁺ 423.1627, found 423.1622.

*5.1.21 N-(2-((2-(6-(difluoromethyl)-1H-indazol-3-yl)-1H-indol-4-yl)oxy)ethyl)-2-fluoroacetamide (**35**)*

^{1}H NMR (400 MHz, DMSO-*d$_6$*) δ 13.60 (s, 1H), 11.65 (s, 1H), 8.45 (t, *J* = 5.9 Hz, 1H), 8.31 (d, *J* = 8.5 Hz, 1H), 7.85 (s, 1H), 7.44 (d, *J* = 8.6 Hz, 1H), 7.22 (t, *J* = 55.8 Hz, 1H), 7.18 – 7.01 (m, 3H), 6.55 (d, *J* = 7.4 Hz, 1H), 4.93 (s, 1H), 4.81 (s, 1H), 4.19 (t, *J* = 5.9 Hz, 2H), 3.65 (q, *J* = 6.0 Hz, 2H). ^{13}C NMR (101 MHz, DMSO-*d$_6$*) δ 167.96 (d, *J* = 18.3 Hz), 152.29, 141.06, 138.46, 138.25, 132.68 (t, *J* = 22.1 Hz), 130.04, 123.21, 122.04, 121.45, 119.81, 118.27, 115.74 (t, *J* = 236.8 Hz), 109.38, 105.66, 101.07, 97.86, 81.44, 79.66, 66.56, 38.43. HRMS (ESI) m/z calcd. for $C_{20}H_{18}F_3N_4O_2$ [M+H]$^+$ 403.1376, found 403.1377.

*5.1.22 2-Chloro-N-(2-((2-(6-(difluoromethyl)-1H-indazol-3-yl)-1H-indol-4-yl)oxy)ethyl)acetamide (**36**)*

^{1}H NMR (400 MHz, MeOD) δ 8.58 (s, 1H), 8.28 (d, *J* = 8.4 Hz, 1H), 7.76 (s, 1H), 7.42 (d, *J* = 8.5 Hz, 1H), 7.20 (s, 1H), 7.11 – 7.05 (m, 2H), 6.86 (t, *J* = 56.2 Hz, 1H), 6.55 (d, *J* = 7.2 Hz, 1H), 4.26 (t, *J* = 5.4 Hz, 2H), 4.11 (s, 2H), 3.76 (t, *J* = 5.3 Hz, 2H). ^{13}C NMR (101 MHz, MeOD) δ 162.90, 152.25, 141.02, 138.27, 133.32, 129.46, 122.73, 121.35, 119.80, 117.72, 115.19, 109.35, 107.93, 104.72, 100.30, 97.73, 66.06, 41.81, 39.34. HRMS (ESI) m/z calcd. for $C_{20}H_{18}ClF_2N_4O_2$ [M+H]+ 419.1081, found 419.1083.

*5.1.23 (E)-N-(2-((2-(6-(difluoromethyl)-1H-indazol-3-yl)-1H-indol-4-yl)oxy)ethyl)but-2-enamide (**37**)*

^{1}H NMR (500 MHz, Acetone-*d$_6$*) δ 12.72 (s, 1H), 10.80 (s, 1H), 8.35 (d, *J* = 8.4 Hz, 1H), 7.91 (s, 1H), 7.55 – 7.50 (m, 2H), 7.28 (d, *J* = 2.2 Hz, 1H), 7.23 – 6.94 (m, 3H), 6.89 – 6.77 (m, 1H), 6.60 (d, *J* = 7.7 Hz, 1H), 6.06 (dd, *J* = 15.2, 1.9 Hz, 1H), 4.28 (t, *J* = 5.6 Hz, 2H), 3.81 (q, *J* = 5.6 Hz, 2H), 1.81 (dd, *J* = 6.8, 1.6 Hz, 3H). 13C NMR (126 MHz, Acetone-*d$_6$*) δ 165.44, 152.56, 141.20, 138.58, 138.25, 133.05 (t, J = 22.1 Hz), 129.76, 125.77, 123.18, 121.60, 121.53, 120.04, 118.08 (t, J = 5.0 Hz), 115.41 (t, J = 236.6 Hz), 108.59 (t, J = 7.6 Hz), 104.98, 100.63, 98.03, 66.79, 38.79, 16.76. HRMS (ESI) m/z calcd. for $C_{22}H_{21}F_2N_4O_2$ [M+H]$^+$ 411.1627, found 411.1625.

*5.1.24 (E)-N-(2-((2-(6-(difluoromethyl)-1H-indazol-3-yl)-1H-indol-4-yl)oxy)ethyl)-4,4,4-trifluorobut-2-enamide (**38**)*

^{1}H NMR (400 MHz, MeOD) δ 8.26 (d, *J* = 8.5 Hz, 1H), 7.75 (s, 1H), 7.42 (d, *J* = 8.6 Hz, 1H), 7.19 (d, *J* = 0.8 Hz, 1H), 7.12 – 7.05 (m, 2H), 6.98 (t, *J* = 46.9 Hz, 1H), 6.85 – 6.72 (m, 2H), 6.55 (dd, *J* = 7.2, 1.3 Hz, 1H), 4.28 (t, *J* = 5.3 Hz, 2H), 3.82 (t, *J* = 5.3 Hz, 2H). ^{13}C NMR (126 MHz, MeOD) δ 163.83, 152.23, 140.97, 138.60, 138.26, 133.48, 133.30, 133.12, 131.48, 131.43, 131.38, 131.34, 129.56, 129.47, 127.42, 127.14, 126.87, 126.59, 124.78, 123.87, 122.72, 121.73, 121.35, 121.30, 119.74, 117.75, 117.71, 117.67, 117.08, 115.20, 113.31, 107.92, 104.73, 100.18, 97.70, 78.13, 77.87, 77.61, 66.06, 60.14, 39.38. HRMS (ESI) m/z calcd. for $C_{22}H_{18}F_5N_4O_2$ [M+H]$^+$ 465.1344, found 465.1346.

5.1.25

*(E)-N-(2-((2-(6-(difluoromethyl)-1H-indazol-3-yl)-1H-indol-4-yl)oxy)ethyl)-4-(dimethylamino)but-2-enamide (**39**)*

^{1}H NMR (500 MHz, MeOD) δ 8.28 (d, *J* = 8.4 Hz, 1H), 7.78 (s, 1H), 7.43 (d, *J* = 8.5 Hz, 1H), 7.26 – 7.06 (m, 3H), 6.94 (t, *J* = 56.2 Hz, 1H), 6.74 (dt, *J* = 14.9, 7.3 Hz, 1H), 6.55 (d, *J* = 7.3 Hz, 1H), 6.44 (d, *J* = 15.3 Hz, 1H), 4.28 (t, *J* = 5.2 Hz, 2H), 3.86 (d, *J* = 7.3 Hz, 2H), 3.82 (t, *J* = 5.1 Hz, 2H), 2.82 (s, 6H). ^{13}C NMR (126 MHz, MeOD) δ 165.28, 152.29, 140.99, 138.27, 133.32 (t, *J* = 22.2 Hz), 132.34, 129.93, 129.36, 128.53, 127.83, 122.79, 121.31, 119.64, 117.70 (t, *J* = 5.0 Hz), 115.22 (t, *J* = 237.0 Hz), 108.07 (t, *J* = 7.2 Hz), 104.73, 100.16, 97.73, 66.14, 57.39, 41.76, 39.24. HRMS (ESI) m/z calcd. for $C_{24}H_{26}F_2N_5O_2$ [M+H]$^+$ 454.2049, found 454.2046.

*5.1.26 N-(2-((2-(6-(difluoromethyl)-1H-indazol-3-yl)-1H-indol-4-yl)oxy)ethyl)but-2-ynamide (**40**)*

^{1}H NMR (400 MHz, Acetone-*d$_6$*) δ 12.66 (s, 1H), 10.79 (s, 1H), 8.36 (d, *J* = 8.6 Hz, 1H), 7.97 – 7.86 (m, 2H), 7.51 (dd, *J* = 8.4, 1.2 Hz, 1H), 7.30 (dd, *J* = 2.3, 0.9 Hz, 1H), 7.26 – 6.93 (m, 3H), 6.59 (d, *J* = 7.7 Hz, 1H), 4.27 (t, *J* = 5.6 Hz, 2H), 3.77 (d, *J* = 5.7 Hz, 2H), 1.91 (s, 3H). ^{13}C NMR (101 MHz, Acetone-*d$_6$*) δ 153.07, 152.50, 141.19, 138.59, 138.24, 133.06 (t, *J* = 22.2 Hz), 129.74, 123.16, 121.59, 120.03, 118.09 (t, *J* = 5.1 Hz), 115.40 (t, *J* = 236.6 Hz), 108.59 (t, *J* = 7.6 Hz), 105.01, 100.54, 98.05, 81.76, 75.25, 66.40, 66.32, 39.00, 2.21. HRMS (ESI) m/z calcd. for $C_{22}H_{19}F_2N_4O_2$ [M+H]$^+$ 409.1471, found 409.1468.

5.1.27

*N-(2-((2-(6-(difluoromethyl)-1H-indazol-3-yl)-6-(hydroxydiphenylmethyl)-1H-indol-4-yl)oxy)ethyl)acrylamide (**41**)*

^{1}H NMR (400 MHz, MeOD) δ 8.25 (d, *J* = 8.5 Hz, 1H), 7.74 (s, 1H), 7.40 (dd, *J* = 8.5, 1.3 Hz, 1H), 7.35 – 7.20 (m, 10H), 7.17 (d, *J* = 0.9 Hz, 1H), 6.92 (t, *J* = 56.2 Hz, 1H), 6.82 (t, *J* = 1.1 Hz, 1H), 6.60 (d, *J* = 1.3 Hz, 1H), 6.40 – 6.20 (m, 2H), 5.65 (dd, *J* = 9.3, 2.7 Hz, 1H), 4.12 (t, *J* = 5.4 Hz, 2H), 3.72 (d, *J* = 5.3 Hz, 2H). ^{13}C NMR (126 MHz, MeOD) δ 167.07, 151.58, 147.81, 143.01, 140.96, 138.59, 137.35, 133.31 (t, *J* = 22.2 Hz), 130.56, 130.01, 128.01, 127.14, 126.47, 125.50, 118.71, 117.71 (t, *J* = 5.0 Hz), 115.20 (t, *J* = 237.1 Hz), 107.90, 105.48, 101.59, 97.70, 82.31, 66.21, 38.94. ^{19}F NMR (376 MHz, MeOD) δ -110.76. HRMS (ESI) m/z calcd. for $C_{34}H_{28}F_2N_4O_3Na$ [M+Na]$^+$ 601.2022, found 601.2004.

5.1.28

*N-(2-((2-(6-(difluoromethyl)-1H-indazol-3-yl)-6-(hydroxy(phenyl)methyl)-1H-indol-4-yl)oxy)ethyl)acrylamide (**42**)*

^{1}H NMR (400 MHz, MeOD) δ 8.24 (d, *J* = 8.5 Hz, 1H), 7.74 (s, 1H), 7.42 (m, 3H), 7.31 (t, *J* = 7.5 Hz, 2H), 7.21 (t, *J* = 7.3 Hz, 1H), 7.15 (q, *J* = 1.0 Hz, 2H), 6.91 (t, *J* = 56.2 Hz, 1H), 6.57 (d, *J* = 1.1 Hz, 1H), 6.40 – 6.21 (m, 2H), 5.86 (s, 1H), 5.66 (dd, *J* = 9.2, 2.8 Hz, 1H), 4.20 (t, *J* = 5.4 Hz, 2H), 3.75 (t, *J* = 5.4 Hz, 2H). ^{13}C NMR (126 MHz, MeOD) δ 167.09, 152.12, 144.90, 140.96, 140.05, 138.60, 137.97, 133.29 (t, *J* = 22.1 Hz), 130.58, 129.77, 127.75, 126.63, 126.36, 125.49, 121.35, 119.03, 117.68 (t, *J* = 5.0 Hz), 115.20 (t, *J* = 237.0 Hz), 107.89 (t, *J* = 7.3 Hz), 103.11, 99.63, 97.76, 76.33, 66.25, 38.99. HRMS (ESI) m/z calcd. for $C_{28}H_{24}F_2N_4O_3Na$ [M+Na]$^+$ 525.1709, found 525.1706.

*5.1.29 N-(2-((6-benzyl-2-(6-(difluoromethyl)-1H-indazol-3-yl)-1H-indol-4-yl)oxy)ethyl)acrylamide (**43**)*

^{1}H NMR (400 MHz, MeOD) δ 8.25 (d, *J* = 8.5 Hz, 1H), 7.74 (s, 1H), 7.40 (d, *J* = 8.5 Hz, 1H), 7.25 (d, *J* = 5.5 Hz, 4H), 7.19 – 7.12 (m, 2H), 6.93 (s, 1H), 6.92 (t, *J* = 56.2 Hz, 1H), 6.41 (s, 1H), 6.37 – 6.22 (m, 2H), 5.66 (dd, *J* = 9.3, 2.7 Hz, 1H), 4.19 (t, *J* = 5.4 Hz, 2H), 4.04 (s, 2H), 3.75 (t, *J* = 5.4 Hz, 2H). ^{13}C NMR (126 MHz, MeOD) δ 167.11, 152.17, 141.98, 140.96, 138.70, 138.39, 136.81, 133.28 (t, *J* = 22.3 Hz), 130.58, 129.21, 128.52, 127.92, 125.47, 121.38, 118.14, 117.64 (t, *J* = 5.1 Hz), 115.22 (t, *J* = 237.0 Hz), 107.87, 104.77, 101.97, 97.75, 66.22, 42.14, 39.02. HRMS (ESI) m/z calcd. for $C_{28}H_{25}F_2N_4O_2$ [M+H]$^+$ 487.1940, found 487.1939.

5.1.30

*N-(2-((2-(6-(difluoromethyl)-1H-indazol-3-yl)-6-(phenyl((tetrahydro-2H-pyran-4-yl)oxy)methyl)-1H-indol-4-yl)oxy)ethyl)acrylamide (**44**)*

^{1}H NMR (400 MHz, MeOD) δ 8.26 (d, *J* = 8.5 Hz, 1H), 7.75 (s, 1H), 7.47 – 7.37 (m, 3H), 7.36 – 7.27 (m, 2H), 7.26 – 7.19 (m, 1H), 7.16 (s, 2H), 6.92 (t, *J* = 56.2 Hz, 1H), 6.56 (d, *J* = 1.1 Hz, 1H), 6.39 – 6.19 (m, 2H), 5.70 (s, 1H), 5.66 (dd, *J* = 9.2, 2.8 Hz, 1H), 4.20 (t, *J* = 5.4 Hz, 2H), 4.00 – 3.87 (m, 2H), 3.76 (t, *J* = 5.4 Hz, 2H), 3.71 (dt, *J* = 8.7, 4.5 Hz, 1H), 3.43 (ddt, *J* = 11.9, 9.4, 3.3 Hz, 2H), 2.01 – 1.92 (m, 2H), 1.73 – 1.66 (m, 2H). ^{13}C NMR (126 MHz, MeOD) δ 167.11, 152.24, 147.55, 143.33, 140.99, 137.94, 133.30 (t, *J* = 22.3 Hz), 130.57, 129.87, 127.76, 126.75, 126.72, 125.51, 121.34, 119.22, 117.71 (t, *J* = 5.1 Hz), 115.20 (t, *J* = 237.1 Hz), 107.93, 106.44, 103.76, 99.80, 97.77, 80.79, 71.31, 66.28, 65.38, 65.31, 38.98, 37.77, 32.64, 32.08. HRMS (ESI) m/z calcd. for $C_{33}H_{32}F_2N_4O_4Na$ [M+Na]$^+$ 609.2284, found 609.2282.

5.1.31

*N-(2-((6-((but-3-yn-1-yloxy)(phenyl)methyl)-2-(6-(difluoromethyl)-1H-indazol-3-yl)-1H-indol-4-yl)oxy)ethyl)acrylamide (**45**)*

^{1}H NMR (400 MHz, MeOD) δ 8.25 (d, *J* = 8.4 Hz, 1H), 7.74 (s, 1H), 7.42 (d, *J* = 7.2 Hz, 3H), 7.30 (t, *J* = 7.4 Hz, 2H), 7.23 (d, *J* = 8.0 Hz, 1H), 7.14 (d, *J* = 14.6 Hz, 2H), 6.92 (t, *J* = 56.3 Hz, 1H), 6.58 (s, 1H), 6.38 – 6.20 (m, 2H), 5.66 (d, *J* = 9.3 Hz, 1H), 5.52 (s, 1H), 4.20 (d, *J* = 6.4 Hz, 2H), 3.75 (d, *J* = 5.5 Hz, 2H), 3.62 (q, *J* = 6.8 Hz, 2H), 2.53 (d, *J* = 7.5 Hz, 2H), 2.28 (s, 1H). ^{13}C NMR (101 MHz, MeOD) δ 167.14, 152.28, 142.75, 140.99, 138.58, 137.94, 137.48, 133.32 (t, *J* = 22.2 Hz), 130.60, 129.91, 127.75, 126.83, 126.67, 125.44, 121.34, 119.30,

117.71 (t, *J* = 4.9 Hz), 115.18 (t, *J* = 237.2 Hz), 107.88 (t, *J* = 6.6 Hz), 103.80, 99.81, 97.80, 84.24, 81.01, 69.03, 66.88, 66.37, 39.01, 19.27. HRMS (ESI) m/z calcd. for $C_{32}H_{28}F_2N_4O_3Na$ [M+Na]$^+$ 577.2022, found 577.2014.

5.1.32

*N-(2-((2-(6-(difluoromethyl)-1H-indazol-3-yl)-6-((2-(methylsulfonyl)ethoxy)(phenyl)methyl)-1H-indol-4-yl)oxy)ethyl)acrylamide (**46**)*

¹H NMR (400 MHz, MeOD) δ 8.25 (d, *J* = 8.5 Hz, 1H), 7.75 (s, 1H), 7.48 – 7.37 (m, 3H), 7.32 (t, *J* = 7.5 Hz, 2H), 7.28 – 7.19 (m, 1H), 7.15 (d, *J* = 10.0 Hz, 2H), 6.92 (t, *J* = 56.2 Hz, 1H), 6.58 (d, *J* = 1.1 Hz, 1H), 6.38 – 6.21 (m, 2H), 5.66 (dd, *J* = 9.2, 2.9 Hz, 1H), 5.55 (s, 1H), 4.22 (td, *J* = 5.6, 2.3 Hz, 2H), 4.00 – 3.85 (m, 2H), 3.76 (t, *J* = 5.4 Hz, 2H), 3.43 (t, *J* = 4.2 Hz, 2H), 3.07 (s, 3H). ¹³C NMR (126 MHz, MeOD) δ 167.11, 152.39, 142.22, 140.99, 138.48, 137.91, 136.74, 133.30, 130.58, 130.02, 127.94, 127.03, 126.54, 125.52, 121.32, 119.39, 117.73 (t, *J* = 5.0 Hz), 115.20 (t, *J* = 237.2 Hz), 107.94 (t, *J* = 6.7 Hz), 103.74, 99.45, 97.76, 84.98, 66.29, 62.65, 54.62, 41.93, 38.96. HRMS (ESI) m/z calcd. for $C_{31}H_{30}F_2N_4O_5SNa$ [M+Na]$^+$ 631.1797, found 631.1803.

*5.1.33 N-(2-((6-(3-chlorobenzyl)-2-(6-(difluoromethyl)-1H-indazol-3-yl)-1H-indol-4-yl)oxy)ethyl)acrylamide (**47**)*

¹H NMR (400 MHz, MeOD) δ 8.24 (d, *J* = 8.5 Hz, 1H), 7.74 (s, 1H), 7.40 (d, *J* = 8.5 Hz, 1H), 7.28 – 7.20 (m, 2H), 7.20 – 7.11 (m, 3H), 7.09 – 6.72 (m, 2H), 6.40 (d, *J* = 1.2 Hz, 1H), 6.37 – 6.23 (m, 2H), 5.66 (dd, *J* = 9.2, 2.8 Hz, 1H), 4.20 (t, *J* = 5.4 Hz, 2H), 4.02 (s, 2H), 3.75 (t, *J* = 5.4 Hz, 2H). ¹³C NMR (101 MHz, MeOD) δ 167.14, 152.31, 144.45, 140.98, 138.41, 135.83, 133.74, 133.30, 130.60, 129.42, 129.38, 128.43, 126.89, 125.56, 125.44, 121.35, 118.35, 117.66, 115.19, 107.86, 104.88, 102.02, 97.77, 66.31, 41.63, 39.02. HRMS (ESI) m/z calcd. for $C_{28}H_{24}ClF_2N_4O_2$ [M+H]$^+$ 521.1550, found 521.1555.

5.1.34

*N-(2-((2-(6-(difluoromethyl)-1H-indazol-3-yl)-6-(3-(trifluoromethyl)benzyl)-1H-indol-4-yl)oxy)ethyl)acrylamide (**48**)*

¹H NMR (400 MHz, MeOD) δ 8.24 (d, *J* = 8.8 Hz, 1H), 7.74 (s, 1H), 7.54 (s, 1H), 7.53 – 7.36 (m, 4H), 7.15 (s, 1H), 7.07 – 6.73 (m, 2H), 6.42 (d, *J* = 1.2 Hz, 1H), 6.36 – 6.21 (m, 2H), 5.66 (dd, *J* = 9.2, 2.8 Hz, 1H), 4.20 (t, *J* = 5.4 Hz, 2H), 4.11 (s, 2H), 3.75 (t, *J* = 5.4 Hz, 2H). ¹³C NMR (126 MHz, MeOD) δ 167.12, 152.36, 143.46, 140.97, 138.62, 138.40, 135.63, 133.29 (t, *J* = 22.1 Hz), 132.29, 130.57, 130.31, 130.06, 129.44, 128.68, 125.50, 124.97 (q, *J* = 3.8 Hz), 124.97 (q, *J* = 3.8 Hz), 121.36, 118.37, 117.67 (t, *J* = 5.1 Hz), 115.21 (t, *J* = 237.1 Hz), 107.90, 104.89, 101.86, 97.76, 66.25, 41.68, 38.99. HRMS (ESI) m/z calcd. for $C_{29}H_{24}F_5N_4O_2$ [M+H]$^+$ 555.1814, found 555.1819.

*5.1.35 N-(2-((2-(6-(difluoromethyl)-1H-indazol-3-yl)-6-(3-methylbenzyl)-1H-indol-4-yl)oxy)ethyl)acrylamide (**49**)*

¹H NMR (400 MHz, MeOD) δ 8.25 (d, *J* = 8.4 Hz, 1H), 7.74 (s, 1H), 7.40 (d, *J* = 9.2 Hz, 1H), 7.22 – 7.10 (m, 2H), 7.07 – 7.01 (m, 2H), 7.01 – 6.75 (m, 3H), 6.40 (d, *J* = 1.2 Hz, 1H), 6.38 – 6.18 (m, 2H), 5.66 (dd, *J* = 9.3, 2.7 Hz, 1H), 4.20 (t, *J* = 5.4 Hz, 2H), 3.99 (s, 2H), 3.75 (t, *J* = 5.4 Hz, 2H), 2.28 (s, 3H). ¹³C NMR (126 MHz, MeOD) δ 167.19, 152.12, 141.86, 140.95, 138.70, 138.38, 137.54, 136.99, 133.30 (t, *J* = 22.3 Hz), 130.54, 129.22, 129.16, 127.83, 126.16, 125.60, 121.40, 121.30, 118.09, 117.68 (t, *J* = 5.0 Hz), 115.21 (t, *J* = 237.1 Hz), 107.91 (t, *J* = 7.7 Hz), 104.78, 102.04, 97.77, 66.24, 42.08, 39.03, 20.10. HRMS (ESI) m/z calcd. for $C_{29}H_{27}F_2N_4O_2$ [M+H]$^+$ 501.2097, found 501.2092.

*5.1.36   N-(2-((2-(6-(difluoromethyl)-1H-indazol-3-yl)-6-(2-methoxybenzyl)-1H-indol-4-yl)oxy)ethyl)acrylamidee (**50**)*

¹H NMR (400 MHz, MeOD) δ 8.23 (d, *J* = 8.6 Hz, 1H), 7.73 (s, 1H), 7.39 (d, *J* = 8.5 Hz, 1H), 7.21 – 7.07 (m, 3H), 7.07 – 6.75 (m, 4H), 6.44 (s, 1H), 6.38 – 6.20 (m, 2H), 5.66 (dd, *J* = 9.3, 2.7 Hz, 1H), 4.19 (t, *J* = 5.3 Hz, 2H), 4.01 (s, 2H), 3.82 (s, 2H), 3.75 (t, *J* = 5.3 Hz, 3H). ¹³C NMR (126 MHz, MeOD) δ 167.16, 157.34, 151.95, 140.96, 138.76, 138.39, 136.72, 133.29 (t, *J* = 22.3 Hz), 130.55, 130.08, 129.96, 129.01, 126.98, 125.57, 121.41, 120.06, 117.98, 117.65 (t, *J* = 5.1 Hz), 115.21 (t, *J* = 237.2 Hz), 110.13, 107.89 (t, *J* = 7.4 Hz), 104.68, 102.09,

97.76, 66.22, 54.46, 39.05, 38.98, 35.90. HRMS (ESI) m/z calcd. for $C_{29}H_{27}F_2N_4O_3$ [M+H]$^+$ 517.2046, found 517.2049.

5.1.37   N-(2-((2-(6-(difluoromethyl)-1H-indazol-3-yl)-6-(3-methoxybenzyl)-1H-indol-4-yl)oxy)ethyl)acrylamide (51)

^{1}H NMR (400 MHz, MeOD) δ 8.25 (d, *J* = 8.5 Hz, 1H), 7.74 (s, 1H), 7.40 (d, *J* = 8.6 Hz, 1H), 7.23 – 7.12 (m, 2H), 7.10 – 6.70 (m, 5H), 6.42 (d, *J* = 1.2 Hz, 1H), 6.38 – 6.21 (m, 2H), 5.66 (dd, *J* = 9.3, 2.7 Hz, 1H), 4.20 (t, *J* = 5.4 Hz, 2H), 4.01 (s, 2H), 3.77 – 3.74 (m, 5H). ^{13}C NMR (126 MHz, MeOD) δ 167.12, 159.81, 152.16, 143.52, 140.97, 138.70, 138.38, 136.65, 133.29, 130.58, 129.22, 128.85, 125.49, 121.39, 121.31, 120.95, 118.16, 117.64, 115.22 (t, *J* = 236.9 Hz), 114.16, 110.89, 107.88, 104.78, 101.97, 97.75, 66.23, 54.12, 42.14, 39.03. HRMS (ESI) m/z calcd. for $C_{29}H_{27}F_2N_4O_3$ [M+H]$^+$ 517.2046, found 517.2041.

5.1.38   N-(2-((2-(6-(difluoromethyl)-1H-indazol-3-yl)-6-(4-methoxybenzyl)-1H-indol-4-yl)oxy)ethyl)acrylamide (52)

^{1}H NMR (400 MHz, MeOD) δ 8.25 (d, *J* = 8.5 Hz, 1H), 7.74 (s, 1H), 7.40 (d, *J* = 8.5 Hz, 1H), 7.20 – 7.10 (m, 3H), 7.09 – 6.74 (m, 4H), 6.39 (d, *J* = 1.1 Hz, 1H), 6.36 – 6.21 (m, 2H), 5.66 (dd, *J* = 9.3, 2.7 Hz, 1H), 4.19 (t, *J* = 5.4 Hz, 2H), 3.97 (s, 2H), 3.76 – 3.74 (m, 5H). ^{13}C NMR (126 MHz, MeOD) δ 167.10, 157.98, 152.14, 140.96, 138.71, 138.38, 137.33, 134.01, 133.26 (t, *J* = 22.2 Hz), 130.58, 129.43, 129.14, 125.50, 121.38, 121.30, 118.07, 117.63 (t, *J* = 5.0 Hz), 115.22 (t, *J* = 237.1 Hz), 107.87 (t, *J* = 7.6 Hz), 104.64, 101.90, 97.77, 66.73, 66.20, 54.22, 41.24, 39.03. HRMS (ESI) m/z calcd. for $C_{29}H_{27}F_2N_4O_3$ [M+H]$^+$ 517.2046, found 517.2045.

5.1.39 N-(2-((2-(6-(difluoromethyl)-1H-indazol-3-yl)-6-(2,6-dimethoxybenzyl)-1H-indol-4-yl)oxy)ethyl)acrylamide (53)

^{1}H NMR (500 MHz, MeOD) δ 8.23 (d, *J* = 8.4 Hz, 1H), 7.73 (s, 1H), 7.38 (d, *J* = 8.5 Hz, 1H), 7.16 (t, *J* = 8.3 Hz, 1H), 7.10 (s, 1H), 7.06 – 6.78 (m, 2H), 6.63 (d, *J* = 8.3 Hz, 2H), 6.52 (s, 1H), 6.38 – 6.20 (m, 2H), 5.67 (dd, *J* = 9.7, 2.4 Hz, 1H), 4.19 (t, *J* = 5.4 Hz, 2H), 4.05 (s, 2H), 3.82 (s, 6H), 3.76 (t, *J* = 5.3 Hz, 2H). ^{13}C NMR (126 MHz, MeOD) δ 167.10, 158.28, 151.60, 140.94, 138.85, 138.34, 137.43, 133.27 (t, *J* = 22.2 Hz), 130.59, 128.75, 127.04, 125.48, 121.42, 121.29, 117.93, 117.72, 133.27 (t, *J* = 22.2 Hz), 115.22 (t, *J* = 237.1 Hz), 107.83 (t, *J* = 7.6 Hz), 104.14, 103.58, 101.98, 97.72, 66.17, 54.80, 39.09, 28.59. HRMS (ESI) m/z calcd. for $C_{30}H_{29}F_2N_4O_4$ [M+H]$^+$ 547.2151, found 547.2154.

5.1.40 N-(2-((2-(6-(difluoromethyl)-1H-indazol-3-yl)-6-(2,4,6-trimethylbenzyl)-1H-indol-4-yl)oxy)ethyl)acrylamide (54)

^{1}H NMR (400 MHz, MeOD) δ 8.23 (d, *J* = 8.5 Hz, 1H), 7.73 (s, 1H), 7.39 (d, *J* = 8.5 Hz, 1H), 7.12 (d, *J* = 0.9 Hz, 1H), 7.06 – 6.74 (m, 3H), 6.59 (s, 1H), 6.36 (s, 1H), 6.35 – 6.22 (m, 2H), 5.67 (dd, *J* = 9.3, 2.7 Hz, 1H), 4.18 (t, *J* = 5.4 Hz, 2H), 4.11 (s, 2H), 3.75 (t, *J* = 5.4 Hz, 2H), 2.26 (s, 3H), 2.23 (s, 6H). ^{13}C NMR (101 MHz, MeOD) δ 167.12, 152.15, 140.96, 138.53, 136.68, 135.75, 135.10, 134.11, 133.29, 130.60, 128.97, 128.37, 125.47, 121.39, 118.00, 117.62, 115.20, 112.84, 107.84, 103.29, 101.34, 97.80, 66.25, 48.23, 39.05, 34.64, 19.65, 18.90. ^{19}F NMR (376 MHz, MeOD) δ -110.80. HRMS (ESI) m/z calcd. for $C_{31}H_{30}F_2N_4O_2Na$ [M+Na]$^+$ 551.2229, found 551.2227.

5.1.41 N-(2-((2-(6-(1H-pyrazol-4-yl)-1H-indazol-3-yl)-6-benzyl-1H-indol-4-yl)oxy)ethyl)acrylamide (55)

^{1}H NMR (600 MHz, MeOD) δ 8.11 (d, *J* = 8.5 Hz, 1H), 8.06 (s, 1H), 7.71 (s, 1H), 7.50 (dd, *J* = 8.5, 1.4 Hz, 1H), 7.39 – 7.32 (m, 1H), 7.30 – 7.20 (m, 4H), 7.15 (tt, *J* = 5.8, 2.6 Hz, 1H), 7.11 (s, 1H), 6.93 (s, 1H), 6.41 (s, 1H), 6.35 – 6.21 (m, 2H), 5.67 (dd, *J* = 9.8, 2.2 Hz, 1H), 4.20 (t, *J* = 5.4 Hz, 2H), 4.04 (s, 2H), 3.76 (t, *J* = 5.4 Hz, 2H). ^{13}C NMR (151 MHz, MeOD) δ 167.13, 152.12, 142.42, 142.01, 138.36, 136.65, 131.62, 130.60, 129.62, 129.38, 128.52, 127.92, 126.84, 126.58, 125.46, 120.96, 119.82, 118.92, 118.17, 105.64, 104.77, 102.04, 97.54, 66.23, 42.14, 39.04. HRMS (ESI) m/z calcd. for $C_{30}H_{26}N_6O_2Na$ [M+Na]$^+$ 525.2009, found 525.2012.

5.2 Pharmacological assays

5.2.1 Enzymatic assays

The enzymatic activities against ITK, BTK, JAK3, and EGFR were tested with the HTRF$^{®}$ KinEASE™-STK kit (Cisbio Bioassays). All protocols are available from the supplier.

5.2.2 Time-Dependent Assay.

Compounds **1**, **43** and **55** were preincubated with recombinant ITK for different periods of time (0, 5, 10, 15, 20, 30, 45 or 60 min) before ATP was added, and then the substrate was added to initiate the kinase reaction. The following operations were identical to the routine enzymatic activity determination procedures. The inhibition percentage values were plotted versus preincubation time using GraphPad Prism software.

5.2.3 Cellular phosphorylation assay

Jurkat or H9 cells were starved for 1 h. Then, cells were incubated with ITK inhibitors or DMSO for 2 h at 37 °C. 2×10^{6} Jurkat or H9 cells were seeded into a 6-well plate and treated with compounds for 2 h. After stimulation with anti-CD3/CD28 beads for 15 min, cells were collected and lysed in a cell lysis buffer containing protease and phosphatase inhibitors. Western blot analyses were then conducted after separation by SDS/PAGE electrophoresis and transfer to nitrocellulose membranes.

5.2.4 Washout Experiment.

Jurkat cells were starved for 1 h and treated with compounds for 2 h. For washout groups, cells were washed extensively with PBS. The non-washout groups were kept constant as stated above. Cells were stimulated with anti-CD3/CD28 beads for 15 min, lysed, and subjected to standard western blot.

5.2.5 Cell viability and apoptosis assays

Jurkat, H9, Molt-4, and CCRF-CEM cells were cultured in RPMI-1640 (Gibco) supplemented with 1% penicillin-streptomycin and 10% fetal bovine serum (FBS, Gibco). The antiproliferative activity of synthetic compounds was determined by using a CellTiter-Glo® luminescent cell visibility assay (Promega, G7570). Cells were seeded in 96-well plates (5000 cells per well), treated with DMSO and various concentrations of compounds, and then incubated in a CO_2 incubator for 72 h. The detection reagent was added to the culture mixture at room temperature. After 1 h, luminescence was read by using an Envision plate reader Envision 2104. GraphPad Prism was used to analyze the data, forming dose–response curves. The GI_{50} values were the means of triplicate measurements.

5.3 Computational Methods.

5.3.1 Molecular docking study

Docking was performed with Molecular Operating Environment software (MOE, 2015). Hydrogen atoms were added to the ITK–ligand complexes at physiological pH (7.0) with the Protonate 3D tool implemented in MOE. Default Protonate 3D settings were used.

5.3.2 Binding energy

To investigate the electron-withdrawing and donating effects for edge-to-face effects between Phe437 and variously substituted benzyl indoles, we performed calculations using Gaussian 16 [33]. The interaction energies were obtained using the basis set superposition error (BSSE)-corrected calculations. The relative interaction energies in water were obtained using PCM. The conformation optimization and relative energies were determined using M06-2X-D3 methods.

Supporting Information

Kinase selectivity profile for compound **43** and NMR spectra data of compounds.

[1]   H. Mano, Tec family of protein-tyrosine kinases: an overview of their structure and function, Cytokine Growth Factor Rev., 10 (1999) 267-280.

[2]   M. Felices, M. Falk, Y. Kosaka, L.J. Berg, Tec Kinases in T Cell and Mast Cell Signaling, Adv. Immunol., 93 (2007) 145-184.

[3]   K.Q. Liu, S.C. Bunnell, C.B. Gurniak, L.J. Berg, T Cell Receptor–initiated Calcium Release Is Uncoupled from Capacitative Calcium Entry in Itk-deficient T Cells, J. Exp. Med., 187 (1998) 1721-1727.

[4]   E.M. Schaeffer, J. Debnath, G. Yap, D. McVicar, X.C. Liao, D.R. Littman, A. Sher, H.E. Varmus, M.J. Lenardo, P.L. Schwartzberg, Requirement for Tec Kinases Rlk and Itk in T Cell Receptor Signaling and Immunity, Science, 284 (1999) 638-641.

[5]   P.L. Schwartzberg, L.D. Finkelstein, J.A. Readinger, TEC-family kinases: regulators of T-helper-cell differentiation, Nat. Rev. Immunol., 5 (2005) 284-295.

[6]   Y.H. Kim, H.L. Liu, S. Mraz-Gernhard, A. Varghese, R.T. Hoppe, Long-term outcome of 525 patients with mycosis fungoides and Sezary syndrome: clinical prognostic factors and risk for disease progression, Arch. Dermatol., 139 (2003) 857-866.

[7]   D.I. Marks, E.M. Paietta, A.V. Moorman, S.M. Richards, G. Buck, G. DeWald, A. Ferrando, A.K. Fielding, A.H. Goldstone, R.P. Ketterling, M.R. Litzow, S.M. Luger, A.K. McMillan, M.R. Mansour, J.M. Rowe, M.S. Tallman, H.M. Lazarus, T-cell acute lymphoblastic leukemia in adults: clinical features, immunophenotype, cytogenetics, and outcome from the large randomized prospective trial (UKALL XII/ECOG 2993), Blood, 114 (2009) 5136-5145.

[8]   C. Mueller, A. August, Attenuation of Immunological Symptoms of Allergic Asthma in Mice Lacking the Tyrosine Kinase ITK, J. Immunol., 170 (2003) 5056-5063.

[9]   J.A. Readinger, G.M. Schiralli, J.K. Jiang, C.J. Thomas, A. August, A.J. Henderson, P.L. Schwartzberg, Selective targeting of ITK blocks multiple steps of HIV replication, Proc. Natl. Acad. Sci. U. S. A., 105 (2008) 6684-6689.

[10] A. Hussain, L. Yu, R. Faryal, D.K. Mohammad, A.J. Mohamed, C.I. Smith, TEC family kinases in health and disease - loss-of-function of BTK and ITK and the gain-of-function fusions ITK-SYK and BTK-SYK, FEBS J., 278 (2011) 2001-2010.

[11] R.M. Linka, S.L. Risse, K. Bienemann, M. Werner, Y. Linka, F. Krux, C. Synaeve, R. Deenen, S. Ginzel, R. Dvorsky, M. Gombert, A. Halenius, R. Hartig, M. Helminen, A. Fischer, P. Stepensky, K. Vettenranta, K. Köhrer, M.R. Ahmadian, H.J. Laws, B. Fleckenstein, H. Jumaa, S. Latour, B. Schraven, A. Borkhardt, Loss-of-function mutations within the IL-2 inducible kinase ITK in patients with EBV-associated lymphoproliferative diseases, Leukemia, 26 (2012) 963-971.

[12] N. Jain, B. Miu, J.K. Jiang, K.K. McKinstry, A. Prince, S.L. Swain, D.L. Greiner, C.J. Thomas, M.J. Sanderson, L.J. Berg, J. Kang, CD28 and ITK signals regulate autoreactive T cell trafficking, Nat. Med., 19 (2013) 1632-1637.

[13] W. Guo, R. Liu, Y. Ono, A.-H. Ma, A. Martinez, E. Sanchez, Y. Wang, W. Huang, A. Mazloom, J. Li, J. Ning, E. Maverakis, K.S. Lam, H.J. Kung, Molecular characteristics of CTA056, a novel interleukin-2-inducible T-cell kinase inhibitor that selectively targets malignant T cells and modulates oncomirs, Mol. Pharmacol., 82 (2012) 938-947.

[14] I. Bustos-Villalobos, J.W. Bergstrom, N.E. Haigh, J.I. Luna, A. Mitra, A.I. Marusina, A.A. Merleev, E.A. Wang, A. Sukhov, H. Sultani, ITK inhibition for the targeted treatment of CTCL, J. Dermatol. Sci., 87 (2017) 88-91.

[15] J. Das, J.A. Furch, C. Liu, R.V. Moquin, J. Lin, S.H. Spergel, K.W. McIntyre, D.J. Shuster, K.D. O'Day, B. Penhallow, C.Y. Hung, A.M. Doweyko, A. Kamath, H. Zhang, P. Marathe, S.B. Kanner, T.A. Lin, J.H. Dodd, J.C. Barrish, J. Wityak, Discovery and SAR of 2-amino-5-(thioaryl)thiazoles as potent and selective Itk inhibitors, Bioorg. Med. Chem. Lett., 16 (2006) 3706-3712.

[16] J. Das, C. Liu, R.V. Moquin, J. Lin, J.A. Furch, S.H. Spergel, A.M. Doweyko, K.W. McIntyre, D.J. Shuster, K.D. O'Day, B.

Penhallow, C.Y. Hung, S.B. Kanner, T.A. Lin, J.H. Dodd, J.C. Barrish, J. Wityak, Discovery and SAR of 2-amino-5-[(thiomethyl)aryl]thiazoles as potent and selective Itk inhibitors, Bioorg. Med. Chem. Lett., 16 (2006) 2411-2415.

[17] J.-D. Charrier, A. Miller, D.P. Kay, G. Brenchley, Discovery and Structure–Activity Relationship of 3-Aminopyrid-2-ones as Potent and Selective Interleukin-2 Inducible T-Cell Kinase (Itk) Inhibitors, J. Med. Chem., 54 (2011) 2341-2350.

[18] J.-D. Charrier, R.M.A. Knegtel, Advances in the design of ITK inhibitors, Expert Opin. Drug Discovery, 8 (2013) 369-381.

[19] C.W. Zapf, B.S. Gerstenberger, L. Xing, D.C. Limburg, D.R. Anderson, N. Caspers, S. Han, A. Aulabaugh, R. Kurumbail, S. Shaky, X. Li, V. Spaulding, R.M. Czerwinski, N. Seth, Q.G. Medley, Covalent inhibitors of interleukin-2 inducible T cell kinase (itk) with nanomolar potency in a whole-blood assay, J. Med. Chem., 55 (2012) 10047-10063.

[20] Y. Zhong, S. Dong, E. Strattan, L. Ren, J.P. Butchar, K. Thornton, A. Mishra, P. Porcu, J.M. Bradshaw, A. Bisconte, T.D. Owens, E. Verner, K.A. Brameld, J.O. Funk, R.J. Hill, A.J. Johnson, J.A. Dubovsky, Targeting interleukin-2-inducible T-cell kinase (ITK) and resting lymphocyte kinase (RLK) using a novel covalent inhibitor PRN694, J. Biol. Chem., 290 (2015) 5960-5978.

[21] J.D. Harling, A.M. Deakin, S. Campos, R. Grimley, L. Chaudry, C. Nye, O. Polyakova, C.M. Bessant, N. Barton, D. Somers, J. Barrett, R.H. Graves, L. Hanns, W.J. Kerr, R. Solari, Discovery of novel irreversible inhibitors of interleukin (IL)-2-inducible tyrosine kinase (Itk) by targeting cysteine 442 in the ATP pocket, J. Biol. Chem., 288 (2013) 28195-28206.

[22] A. Chaikuad, P. Koch, S.A. Laufer, S. Knapp, The Cysteinome of Protein Kinases as a Target in Drug Development, Angew. Chem. Int. Ed. Engl., 57 (2018) 4372-4385.

[23] Q. Liu, Y. Sabnis, Z. Zhao, T. Zhang, Sara J. Buhrlage, Lyn H. Jones, Nathanael S. Gray, Developing Irreversible Inhibitors of the Protein Kinase Cysteinome, Chem. Biol., 20 (2013) 146-159.

[24] G. Tang, L. Liu, X. Wang, Z. Pan, Discovery of 7*H*-pyrrolo[2,3-*d*]pyrimidine derivatives as selective covalent irreversible inhibitors of interleukin-2-inducible T-cell kinase (Itk), Eur. J. Med. Chem., 173 (2019) 167-183.

[25] Sanofi-aventis, Thienopyrazoles, WO2005026175, 2005.

[26] L.R. McLean, Y. Zhang, N. Zaidi, X. Bi, R. Wang, R. Dharanipragada, J.G. Jurcak, T.A. Gillespy, Z. Zhao, K.Y. Musick, Y.M. Choi, M. Barrague, J. Peppard, M. Smicker, M. Duguid, A. Parkar, J. Fordham, D. Kominos, X-ray crystallographic structure-based design of selective thienopyrazole inhibitors for interleukin-2-inducible tyrosine kinase, Bioorg. Med. Chem. Lett., 22 (2012) 3296-3300.

[27] M. Herdemann, A. Weber, J. Jonveaux, F. Schwoebel, M. Stoeck, I. Heit, Optimisation of ITK inhibitors through successive iterative design cycles, Bioorg. Med. Chem. Lett., 21 (2011) 1852-1856.

[28] Japan Tobacco Inc., Indole compound and pharmaceutical use thereof, WO2011065402, 2011.

[29] J.D. Burch, K. Barrett, Y. Chen, J. DeVoss, C. Eigenbrot, R. Goldsmith, M.H. Ismaili, K. Lau, Z. Lin, D.F. Ortwine, A.A. Zarrin, P.A. McEwan, J.J. Barker, C. Ellebrandt, D. Kordt, D.B. Stein, X. Wang, Y. Chen, B. Hu, X. Xu, P.W. Yuen, Y. Zhang, Z. Pei, Tetrahydroindazoles as interleukin-2 inducible T-cell kinase Inhibitors. Part II. Second-generation analogues with enhanced potency, selectivity, and pharmacodynamic modulation in vivo, J. Med. Chem., 58 (2015) 3806-3816.

[30] J.D. Burch, K. Lau, J.J. Barker, F. Brookfield, Y. Chen, Y. Chen, C. Eigenbrot, C. Ellebrandt, M.H. Ismaili, A. Johnson, D. Kordt, C.H. MacKinnon, P.A. McEwan, D.F. Ortwine, D.B. Stein, X. Wang, D. Winkler, P.W. Yuen, Y. Zhang, A.A. Zarrin, Z. Pei, Property- and structure-guided discovery of a tetrahydroindazole series of interleukin-2 inducible T-cell kinase inhibitors, J. Med. Chem., 57 (2014) 5714-5727.

[31] L.M. Salonen, M. Ellermann, F. Diederich, Aromatic rings in chemical and biological recognition: energetics and structures, Angew. Chem. Int. Ed. Engl., 50 (2011) 4808-4842.

[32] E.A. Meyer, R.K. Castellano, F. Diederich, Interactions with aromatic rings in chemical and biological recognition, Angew. Chem. Int. Ed. Engl., 42 (2003) 1210-1250.

[33] E.C. Lee, B.H. Hong, J.Y. Lee, J.C. Kim, D. Kim, Y. Kim, P. Tarakeshwar, K.S. Kim, Substituent effects on the edge-to-face aromatic interactions, J. Am. Chem. Soc., 127 (2005) 4530-4537.

[34] G. Trani, J.J. Barker, S.M. Bromidge, F.A. Brookfield, J.D. Burch, Y. Chen, C. Eigenbrot, A. Heifetz, M.H.A. Ismaili, A. Johnson, T.M. Krülle, C.H. MacKinnon, R. Maghames, P.A. McEwan, C.A.G.N. Montalbetti, D.F. Ortwine, Y. Pérez-Fuertes, D.G. Vaidya, X. Wang, A.A. Zarrin, Z. Pei, Design, synthesis and structure–activity relationships of a novel class of sulfonylpyridine inhibitors of Interleukin-2 inducible T-cell kinase (ITK), Bioorg. Med. Chem. Lett., 24 (2014) 5818-5823.

[35] T. Barf, A. Kaptein, Irreversible Protein Kinase Inhibitors: Balancing the Benefits and Risks, J. Med. Chem., 55 (2012) 6243-6262.

- A series of indolylindazole based covalent ITK inhibitors were designed and synthesized.
- The most potent compounds, **43** and **55**, inhibited ITK kinase activity with IC_{50} values of 4.0 and 5.8 nM, respectively, and both exhibited good selectivity in a panel of kinases and over 30-fold selectivity against BTK.
- Compounds **43** and **55** potently inhibited the phosphorylation of PLCγ1 and ERK1/2 in living T cells, and showed almost no inhibitory effect on the phosphorylation of PLCγ2 in B cells.